

Stretching a Single Condensed DNA Molecule Studied by Molecular Dynamics Simulation

Paul Antonio Cárdenas Lizana

Submitted to
the Department of Engineering and System Science
at the College of Nuclear Science
in partial fulfillment of the requirements for the degree of
Master of Science

at the

NATIONAL TSING HUA UNIVERSITY

July 2007



Author
Department of Engineering and System Science
College of Nuclear Science
July, 2007

Certified by
Dr. Pai-Yi Hsiao
Assistant Professor
Thesis Supervisor

Accepted by
Chairman, Departmental Committee on Graduate Students



©Copyright By Paul Antonio Cárdenas Lizana 2007
All Rights Reserved.

Abstract

Experiments have shown that a semiflexible polyelectrolyte, such as a DNA, can be condensed by multivalent counterions and the preferred form is toroid. By using molecular dynamics simulations, a single DNA molecule is condensed into a compact toroid-like structure. DNA is treated as a bead-spring chain, using parameters of dsDNA. The influence of the counterion size and DNA monomer size on the DNA structure is studied. We found that for a DNA monomer size of σ and counterion size of 0.5σ , the complex (DNA plus condensed counterions) forms a well-defined toroidal structure. The dependence of the structure of the condensed DNA on the initial configuration is investigated. We observed that the final conformation does not depend on the initial state. The condensed DNA toroid is then stretched by pulling one end of the chain at various constant velocities to investigate the effects of the pulling velocity on the force-extension curve (FEC). We found that the pulling velocity influences the force profile and the internal structure of the condensed DNA molecule. Moreover, the responses at both DNA ends are different if the pulling velocity is larger than the reference Rouse velocity, V_o . For velocities larger than V_o , the FEC's dependence over the pulling velocity is linear at the DNA end which is moving at constant velocity; nevertheless, these FECs oscillate around a constant force ($\approx 2.5K_B T/\sigma$) at the other end. We found that a pulling velocity equals to $5 \times 10^{-4}\sigma/\tau$ does not perturb the complex. Moreover, the influence of the pulling velocity on the bond length is linear. We observed that the entropic behavior of the DNA molecule is strongly affected by the condensed counterions. The FEC shows a series of "stick-release patterns". It gradually increases with increasing extension and then abruptly decreases; this behavior appears repeatedly and becomes stronger and stronger as the condensed DNA molecule is losing its turns. We showed that these "stick-release patterns" are a consequence of turn-by-turn unfolding of the condensed DNA toroid. The

extensible worm-like chain (EWLC) model is found able to describe qualitatively the behavior of the DNA molecule when its extension is close to the overall contour length. We presented a clear evidence and described the mechanism of why the condensed DNA molecule forms a “stick-release patterns”. Our results provide new microscopic information about the internal structure of a single condensed DNA toroid being stretched and are in qualitative agreement with experiments.

Keywords : Condensed DNA toroid; reentrant condensation; force-extension curve (FEC); extensible worm-like chain (WLC) model; “stick-release patterns”; entropic elasticity; molecular dynamics simulation; non-viral gene therapy; and bioengineering.



Acknowledgments

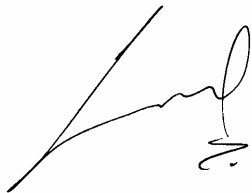
This thesis is the result of two years of my research at Laboratory of Molecular Simulation at the National Tsing Hua University. I wish to express my warmest gratitude to my advisor, Professor Dr. Hsiao Pai-Yi, who originally introduced me into the field of bioengineering and soft condensed matter physics. He initially suggested me to research in “stretching a condensed DNA molecule”. His expertise and the excellent facilities of his laboratory created the basis of this project. I believe that without the many discussions we held on the group meeting and in his office, my apprehension of many concepts and techniques about this project would be much poorer and would not be turned out. The stress-free discussions with him about this project have been a great joy and benefit. I still remember that he always pointed out peculiar aspects of the project, then asked me a lot of questions to make me understand the concept behind the problems. I really appreciate his comments on the numerous drafts of this constantly expanding work and the time he sacrificed in reviewing it. I am also grateful to my colleagues in the laboratory Mr. Wei Yu-Fu, Mr. Wu Kun-Mao, Mr. John Tsai, Mr. Yang Po-Wei, and Mr. Ha Nguyen for much scientific advice on the group meetings and their friendly attitude.

I wish to thank to the official Committee of my thesis defense. I am very grateful to Professor Dr. Long Hsu, from the Nano-Biophotonics Laboratory at National Chiao Tung University, for carefully reading the last version of this manuscript and for his constructive criticism. I am also grateful to Professor Dr. Pik-Yin Lai, from the Statistical Physics and Soft Condensed Matter Laboratory at National Central University, for reading this manuscript and his suggestions on my oral defense.

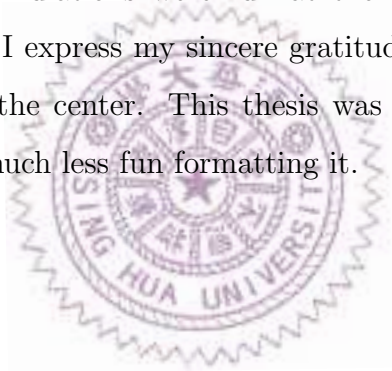
And last but not least by any means, I wish to express my deepest thanks to my family, my dear mother Carmen for her advice, help and never-ending optimism during all this time, my dear father Alejandro for his support and understanding in

all fields of my life, and my dear sister and at the same time my best friend Evelyn who has brought an enormous amount of joy and energy to my life. Without their tireless support and unconditional friendship, I would not have had the courage and the strength to finish this effort. They kept my feet on the ground during the busy and hard days and their cheerfulness created an optimistic atmosphere for this work. I also want to remember my grandmother who has already passed away but she gave me a lesson of life with her courageous attitude to go through any difficulties life had. I also want to thank to my friend Miss Eva Tsai, who helped me a lot during these two years, she made my stay pleasant. I dedicate my thesis to them.

This research was supported by the National Science Council, the Republic of China. Most of the simulations were run at the National Center for High-Performance Computing. I express my sincere gratitude to the members and the staffs of the council and the center. This thesis was written in L^AT_EX, without which I would have had much less fun formatting it.



Paul Cárdenas Lizana.
The Republic of China, July 2007.



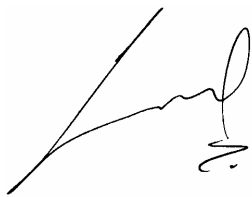
Agradecimientos

Esta tesis es el resultado de dos años de mi investigación en el Laboratorio de Simulación Molecular en la Universidad Nacional Tsing Hua. Desearía expresar mi mas afectuosa gratitud hacia mi asesor, Profesor Dr. Hsiao Pai-Yi, quien originalmente me introdujo en el campo de la bioingeniería y de la física de la materia blanda y condensada. El inicialmente me sugirió que investigue “extendiendo una molecula condensada de ADN”. Su experiencia y las excelentes facilidades que ofrece su laboratorio crearon la base de este proyecto. Creo que sin las muchas discusiones que tuvimos en los grupos de investigación como tanto en su oficina, mi apreciación de la mayoría de conceptos y técnicas empleadas en el proyecto habrían sido infructíferas y tal vez insuficientes para ser terminadas. Estas discusiones libres de estrés llenaron el proyecto de mucha alegría y muchos beneficios al mismo tiempo. Aún recuerdo que mi asesor siempre señaló muchos aspectos peculiares e importantes del proyecto, después realizó una serie de preguntas con el objetivo de hacerme entender la física detrás del problema. Realmente aprecio sus comentarios realizados en los numerosos borradores de esta tesis y el tiempo que él sacrificó para poder revisarlos. También estoy muy agradecido con mis colegas del laboratorio Sr. Wei Yu-Fu, Sr. Wu Kun-Mao, Sr. John Tsai, Sr. Yang Po-Wei, y Sr. Ha Nguyen por los muchos consejos científicos que me dieron en los grupos de investigación y también por su actitud amistoza.

Quisiera agradecer al comité oficial de mi examen de grado. Profesor Dr. Long Hsu, del Laboratorio de Biophotonic en la Universidad Nacional Chiao Tung, al cual le estoy muy agradecido por leer cuidadosamente la ultima version de este manuscrito y por sus críticas constructivas. También le estoy agradecido al Profesor Dr. Pik-Yin Lai, del Laboratorio de Física Estadística y Física de la Materia Blanda y Condensada en la Universidad Nacional Central, por leer este manuscrito y sus sugerencias en mi examen oral.

Y por último pero de ninguna manera menos importante, quisiera expresar my más profundo agradecimiento hacia mi familia, mi adorada madre Carmen por sus consejos, su ayuda y su interminable optimismo durante todo este tiempo, mi estimado padre Alejandro por su apoyo y comprensión en todas las etapas de mi vida, y mi querida hermana y a la vez mejor amiga Evelyn la que trajo una enorme cantidad de alegría y energía a mi vida. Sin sus incansables apoyos e incondicionales amistades, yo no habría tenido el coraje ni la fuerza para terminar este proyecto. Ellos me mantuvieron despierto durante los días atareados y difíciles y sus entusiasmos crearon un ambiente optimístico para este trabajo. También quisiera recordar a mi abuelita, quien ya ha fallecido, pero me dio una lección de vida con su actitud valiente para afrontar cualquier dificultad que la vida tuvo. Quisiera también agradecer a mi amiga Srt. Eva Tsai quien me ayudó bastante durante estos dos años, ella hizo mi estadía muy placentera. Son a ellos a quienes dedico esta tesis.

Esta investigación fue auspiciada por el Consejo Nacional de la Ciencia de la República de China. La mayoría de las simulaciones fueron corridas en el Centro Nacional para la computación de alta performance. Expreso mi más sincera gratitud hacia los miembros y el personal del Consejo y del Centro. Esta tesis fue escrita en L^AT_EX, sin el cual hubiera tenido mucho menos diversión para formatearla.



Paul Cárdenas Lizana.
La República de China, Julio 2007.

Contents

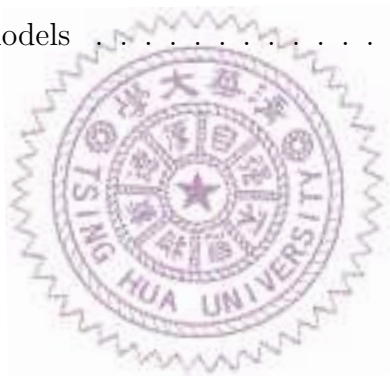
Abstract	3
Acknowledgments	5
Agradecimientos	7
Table of Contents	9
List of Tables	12
List of Figures	13
1 Introduction	15
1.1 Motivation	16
1.2 Reentrant condensation of DNA molecule	20
1.3 Morphology of a condensed DNA molecule	22
1.4 Present research	24
2 Simulation Method and Setup	27
2.1 DNA structure	27
2.2 Coarse-grained model	30
2.3 Molecular dynamics	32
2.4 Force fields	33
2.4.1 Non-bonded interactions	33
2.4.2 Bonded interactions	35
2.5 Integration algorithm	36

2.6	Simulation setup	36
3	Results and Discussions	39
3.1	Toroidal structure of a single condensed DNA molecule	39
3.1.1	Gyration tensor	41
3.1.2	Asphericity	41
3.2	Counterion size	42
3.3	Size and shape of a condensed DNA molecule	45
3.3.1	Gyration tensor	45
3.3.2	The winding number	48
3.4	Stretching process and pulling velocity	49
3.4.1	Stretching process	51
3.4.2	Pulling velocity	52
3.5	Force-extension curve (FEC)	58
3.5.1	N_L and N_R	59
3.5.2	Stick-release behavior	61
3.5.3	Asphericity	70
3.5.4	Minor radius, r_o , and major radius, R	72
3.5.5	Effective fractional extension, x/L_{eff}	74
3.6	How do our results depend on different initial configuration?	76
3.7	Snapshots of our condensed DNA toroid during the stretching process	77
4	Conclusion	79
	Appendix	83
A	The Worm-Like Chain	84
A.1	Theory	84
A.2	Experimental results and their models	86



List of Tables

3.1	DNA monomer and counterion diameter.	43
3.2	Parameters of the condensed DNA toroid calculated at the equilibrium state.	51
3.3	The pulling velocity expressed in σ/τ units.	53
A.1	DNA elasticity models	87



List of Figures

1-1	Schematic plots of the elastic responses of a single condensed DNA for different counterion concentration, C	17
1-2	(a)The dependence of the effective contour length on the DNA's extension. (b) Schematic illustration of the intramolecular phase segregated chain for the "stick-release" case	19
1-3	Percentage of DNA in solution vs counterion concentration	21
1-4	Transmission electron microscopic photographs of collapsed T4 DNA	23
2-1	Atomistic structure of the DNA molecule.	29
2-2	How to coarse grain a DNA molecule and its counterion.	31
2-3	DNA molecule and its coarse grained model. a)A short DNA molecule represented with an atomistic model. b) A coarse grained model of the DNA molecule.	31
3-1	Characteristic parameters of a toroid (a) in 2D projection and (b) in 3D.	40
3-2	Asphericity plotted for each case in the table 3.1 before filtering the noise.	44
3-3	Asphericity illustrated for the cases in the table 3.1	46
3-4	Final values of R_1, R_2 and r_0 as a function of the initial spiral radius.	47
3-5	(a) Snapshot of a DNA in the equilibrium state. (b) Schematic illustration of a toroid.	48

3-6	As and W as a function of the initial spiral radius.	49
3-7	(a) Evolution of a DNA molecule during the simulation. (b) Condensed DNA toroid after reaching the equilibrium state.	50
3-8	Snapshot of a single condensed DNA toroid being stretched.	53
3-9	Force-Extension Curve without applying filter	55
3-10	FEC vs. Pulling velocity	56
3-11	FEC vs. Pulling velocity at one DNA end	57
3-12	Bond length vs. Pulling velocity at the other end	59
3-13	BL_x vs. DNA monomer.	62
3-14	N_L and N_R as a function of the DNA extension	63
3-15	Number of monomers in each part of the DNA molecule.	63
3-16	Winding number calculated by two methods	64
3-17	Condensed DNA molecule and its simplified DNA model of the stretching process	65
3-18	Bond length vs. Winding number	67
3-19	Response of single condensed dsDNA molecule to an applied force.	68
3-20	FEC fitted with the EWLC.	70
3-21	Asphericities plotted for the three parts: part I (rod), part II (toroid) and part III (rod).	71
3-22	Asphericity in the toroid-like structure (part II), calculated by two methods.	71
3-23	Internal parameters of a DNA during the stretching process	73
3-24	Effective contour length plotted for the three parts: part I (rod), part II (toroid) and part III (rod).	75
3-25	The effective fractional extension plotted with the winding number.	75
3-26	Winding numbers plotted together with different initial configurations.	76
3-27	Snapshots of a single condensed DNA toroid during a stretching process.	78

Chapter 1

Introduction

Perhaps the long history of DNA began with its discovery in 1869 by Friedrich Miescher [1]. He found in the cell nucleus a mixture of compounds that he called nuclein. The term “nuclein” was used because these molecules were found in the nucleus of a living cell. The major component of nuclein is deoxyribonucleic acid (DNA). More than 80 years later, Crick and Watson reported to discover the DNA structure by proposing a double helix as a model [2]. Although the structure of the double helix is already known for a such long time, many of its phenomena are not well understood. Indeed, the molecule of life exhibits intriguing phenomena because of its dual character as a highly charged chain and as a semiflexible chain. Most of these intriguing phenomena are strongly dependent on electrostatic interactions between the negative charges on the DNA molecule and the surrounding positively charged counterions, which interact through long range Coulomb forces. The combination of this Coulomb interaction and the specific chemical interactions (stiffness, rigidity, etc.) leads to a diversity of phenomena which are difficult to handle by analytical methods such as mean-field approximations and variational methods.

1.1 Motivation

The main interest for understanding DNA condensation, DNA decondensation, and the process involves between these two transitions is its biological implications in non-viral gene therapy [3, 4] and the benefits that this carries with it. Gene therapy is aimed to treat human diseases ranging from inherited genetic disorders to cancer. Polyamide such as a spermidine and spermine are abundant in living cells and are believed to aid in the DNA condensation, which is a prerequisite for transport of the gene vectors in living cells. DNA condensation should be fast, effective, easily reversible without damaging the DNA molecule. Moreover, if one can control the process of DNA condensation, one is able to pack, deliver, release and insert a “normal” gene from vehicle to a target cell, and then this “normal” gene can replace an “abnormal” gene which causes the disease. In spite of a lot of information in the DNA condensation process, there are still many unsolved questions about the DNA condensation in the range of these two transitions (condensation/decondensation).

In order to understand the behavior of a single DNA in the condensed state and quantify the energy needed to condense it, Baumann et al. [5] and Murayama et al. [6, 7] have investigated the elastic properties of a condensed DNA molecule. They have used an optical tweezer to stretch a single condensed DNA. They observed three different responses of a single condensed DNA when it is stretched, see Figure 1-1. Surprisingly, these different behaviors are related to the condensation/decondensation threshold, C_c , C_d , (These quantities are defined in the section 1.2) and they are strongly dependent on the counterion concentration, as well. At very low counterion concentration, DNA is in a coil state and its elastic response can be described by worm-like-chain (WLC) model (See Figure 1-1 (a)), and for a review of WLC model, see appendix A. At intermediate counterion concentration, the measured force-extension curve (FEC) has a “plateau force”, (See Figure 1-1

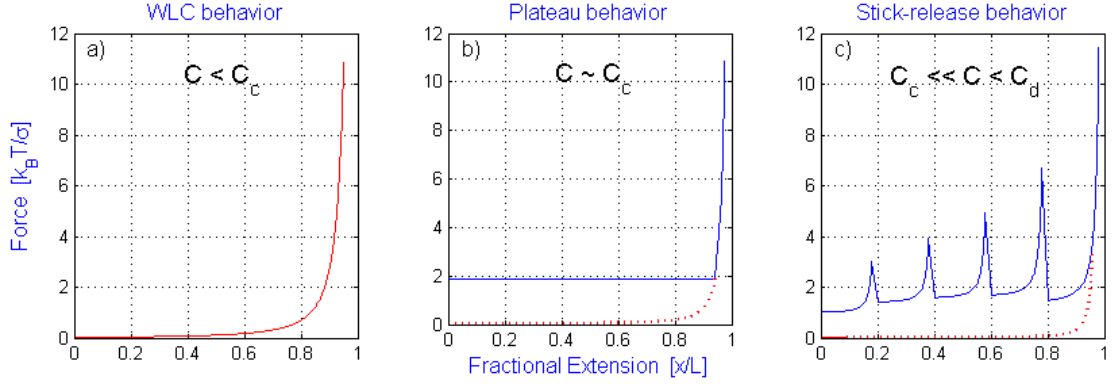


Figure 1-1: Schematic plots of the three typical behaviors of the elastic responses of a single condensed DNA for different values of counterion concentration, C . (a) $C < C_c$. In this regime the DNA molecule behaves as a “worm-like chain”. (b) $C_c \sim C$. The DNA molecule shows a “plateau force” in a wide range of its extension. (c) $C_c \ll C < C_d$. The periodic curve appears, which is known as a “stick-release” behavior. C_c and C_d are the condensed and decondensed concentration of the DNA molecules, respectively.

(b)), which is significantly larger than the force described in the WLC model, and remains unchanged in a wide range of the DNA extension. If the counterion concentration is increased to a high concentration, DNA shows a repeatedly elastic response described by a WLC model at large extension, which is specifically called a “stick-release pattern”, (See Figure 1-1 (c)).

In spite of experimental evidences, current theory can not explain what happened in these experiments, and as a consequence, there is a big gap between theory and experiments. To explain the different FECs, “plateau force” and “stick-release pattern”, researchers have proposed two theories to describe the internal structure of a single condensed DNA molecule when it is stretched. In the first theory, Wada et al. [8] elaborated a numerical model for “plateau force” and “stick-release pattern”. They claimed that “plateau force” can be understood by using the WLC equation. In this equation, the force would be constant, if the ratio of extension, x , to the effective contour length, L_{eff} , are constant. It means that before the DNA molecule becomes elongated (about 86%), the evolution of the fraction extension,

x/L_{eff} , is roughly constant (See Figure 1-2 (a)) and after that, DNA molecule returns to be in a coil state and starts behaving as a WLC model. For the “stick-release pattern”, they based their model on a fluorescence microscopy image of a long DNA [9], which was partially stretched by externally applied electric field. The image shows a group of object loops connected by a line. They argued that the formation of this gripping phenomenon is because the large amount of counterions induce tight condensation of the DNA molecule which forms a united structure, and the “stick-release behavior” appears as a response to abrupt release of condensed objects from the united structure. The condensed objects are a group of “crystallized” globular objects connected with short chain coils (See Figure 1-2 (b)). Moreover, each of these condensed objects has basically a toroidal form. The WLC results from stretching the short chain coils between condensed objects. The periodicity of this “stick-release behavior” was found to be 300 nm [7], which corresponds approximately to the length of the periphery of a toroid, $\approx 2\pi R$, where $R \approx 50\text{ nm}$ is the radius of the toroid. Wada et al. [11] suggested later a new point of view for the formation of “stick-release pattern”, based on experimental and theoretical results [7, 12], which is different from their former formulation. This is the second theory. They argued that “stick-release” behavior can be attributed to turn-by-turn unfolding of the condensed DNA toroid. However, there is no clear evidence to support neither of these models.

Although there is a lot of experimental information about the manipulation on single condensed DNA molecule, there exists only a few theoretical and numerical studies about this combined problem. Our understanding on how condensation of a DNA affects its mechanical properties is still far from satisfactory. The main propose of this research is to study the internal structure of a single condensed DNA and its elastic responses in the stretching process. We measure the FEC to characterize these phenomena. We employ a simple coarse-grained model which

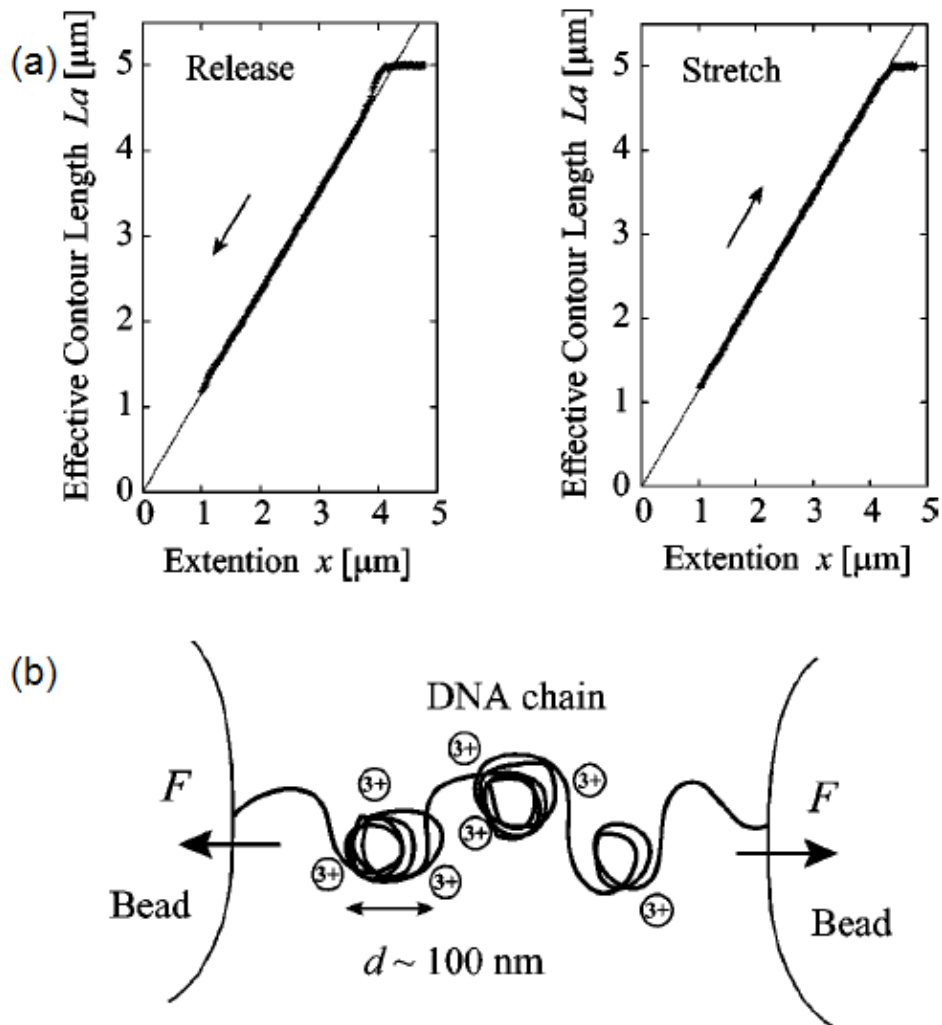


Figure 1-2: (a) The dependence of the effective contour length on the extension in stretching and releasing processes, for the "plateau force" case. (b) Schematic illustration of the intramolecular phase segregated chain for the "stick-release" case. These figures are taken from reference [8]

can reproduce the DNA's behavior. First, we will construct the physical picture for this phenomenon, which is searched for many researchers. Then, we will explain the overall process that can lead to a better understanding when the condensed DNA molecule is stretched.

1.2 Reentrant condensation of DNA molecule

It was understood that for a long DNA, when the concentration of the added condensing agents reaches a critical value, C_c , DNA condensation occurs suddenly. If the concentration of the condensing agent goes far again to another critical values, C_d ($C_c \ll C_d$), DNA molecule dissolves back to the solution (See figure 1-3). This phenomenon is called reentrant condensation [13, 14, 15]. Nguyen et al. [14] proposed an analytical description of the phenomenon. They explained that condensation can only happen in the range, $C_c \leq C \leq C_d$ because of strong counterion correlations on the surface of the DNA. In this range, the condensed counterions on the chain almost neutralize the chain bare charge, and consequently, the correlation induces a short-range attraction that dominates long-range repulsion, leading to precipitation. Moreover, the optimal condition of this region is in the middle, where the chain charge is effectively neutralized ($C \approx C_o$). At high counterion concentration, ($C_d < C$), the repulsion makes difficult chain condensation, and therefore, the DNA molecules redissolve back to the solution (See Figure 1-3). This phenomenon is characterize by

$$\frac{\varepsilon}{K_B T} = \frac{1}{4Z^2\xi} \frac{\ln^2(C_o/C)}{\ln(1 + r_{(C)}/r_{DNA})} \quad (1.1)$$

where $\xi = \lambda/b$ is the manning's parameter, $r_{(C)}$ is the screening length, r_{DNA} is the radius of the DNA, and C is the counterion concentration in the bulk. Setting $C = C_c$ and $C = C_d$ in Eq. 1.1 would give two equations. Solving these

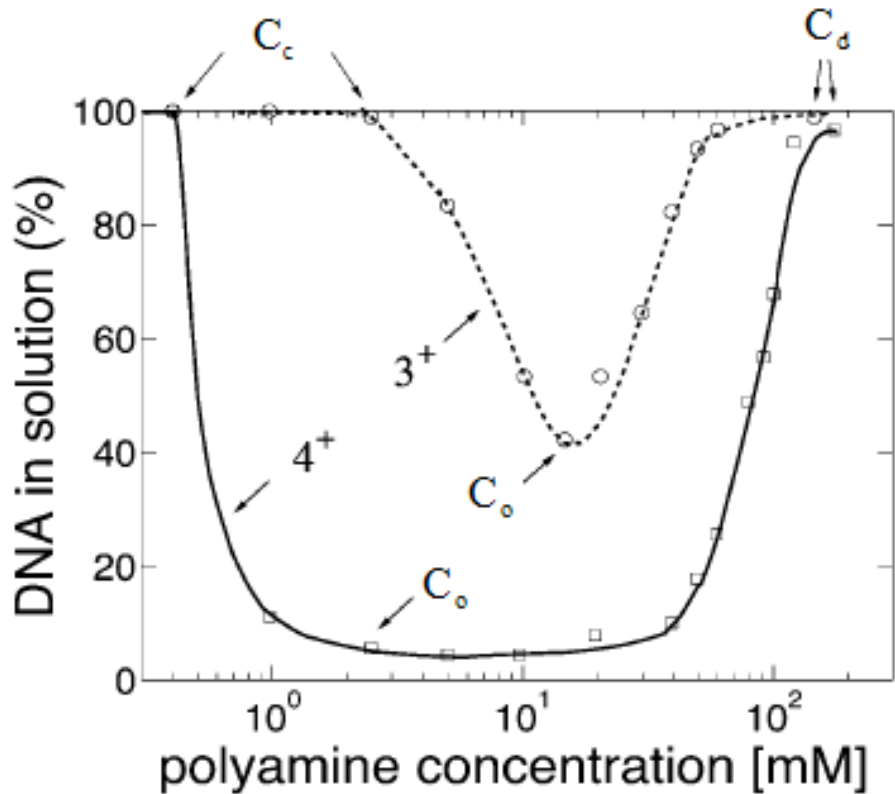


Figure 1-3: Percentage of DNA in solution vs polyamide concentration. The solid and dotted curve show the processes of condensation, ($C \approx C_c$), and decondensation, ($C \approx C_d$), for the spermine and spermidine, respectively. The point, $C = C_o$, corresponds to the neutralizing point. At this point the DNA molecule is effectively neutralized. The figure is taken from reference [10]

two equations simultaneously would give one solution for the condensed energy per base pair, ε , and the neutralizing concentration, C_o , under the assumption that the condensed energy is the same at the condensation and decondensation threshold. Although, This theory presents a good qualitative description about the phenomenon, the predictions, which they gave, are not completely coherent with the experiments [5, 6, 7].

1.3 Morphology of a condensed DNA molecule

In gene therapy, a DNA molecule should be condensed to a stable, effectively charge-neutralized structure, otherwise the negative cell membrane would repel the DNA molecule that is injected into the cell for the purpose of gene delivery. If one were to take one DNA molecule from a human cell and stretch it out to its full length, it would be approximately two meters long. It is incredible that such an enormously long molecule can be easily packed into the nucleus. Since DNA molecule has a high density of negative charge, packing DNA requires overcoming an enormous Coulomb repulsion. We define DNA condensation as the union of DNA molecule and multivalent counterions, often with elimination of water from the helix, which form a newly more complex compound, and the consequence is the decrease in the volume of the extended DNA molecule [16]. DNA condensation is very important because it confronts the statistical-mechanical challenge of accounting how a DNA can be confined in a dimension comparable to its persistence length and yet hundreds of times smaller than its overall contour length. It has been shown that cations with valence larger than two are generally required to induce highly packing of DNA in an aqueous solution at room temperature [17]. To explain the stable morphology of a condensed DNA molecule, various competing models have been proposed in which the DNA molecule is organized in concentric rings as a spool [18], in parallel segments joined at sharp kinks [19], or as a toroid [20]. Single polyelectrolytes can collapse from a random coil to a dense conformation. The surface energy plays a significant role in determining the stable structure of a folded compact single polyelectrolyte. For a flexible chain the minimal surface energy is approximately a spherical globule, but for semiflexible chain is a toroid [21]. Indeed, DNA usually forms beautiful nanotoroids(See Figure 1-4) after adding condensing agents to the solution [80, 23], and these nanotoroids are surprisingly monodisperse, having almost alike size, basically independent of the

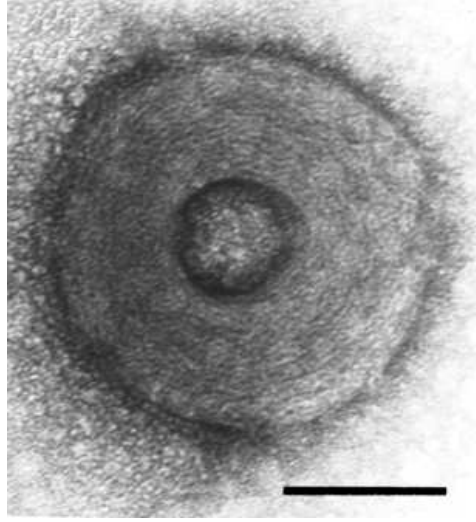


Figure 1-4: Transmission electron microscopic photographs of spermidine-collapsed T4 DNA, giant toroid with 6 mM spermidine, observed At 100 kV. Scale bar is 100 nm. The picture is taken from reference [39]

counterion valence [24, 25]. Researchers studied toroid formation with the help of methods such as light-scattering [27], fluorescence spectroscopy [26], electron microscopy [28] or sedimentation methods [29], and they often used counterions such as spermidine (SPD^{3+}) [30, 31], spermine (SP^{4+}) [26, 27], and hexaamminecobalt complex ($Co(NH_3)_6^{3+}$) [80] to condense a DNA. They have reported that toroidal DNA has typically an outside diameter of $\approx 100\text{ nm}$ with a 30 nm hole [28, 30, 32, 33, 34, 35, 36]. The toroidal form has been shown to be the morphology of DNA packaged within some bacterial phages in prokaryotic and eukaryotic cells [37]. Nowadays, toroid is believed to be the packing shape of a condensed DNA. Owing to a lot of experimental and simulation studies, polyelectrolyte theory has been improved and it has explained that DNA condensation is originated from the correlated fluctuation of condensed counterions on the DNA at close range, which forms a strongly correlated liquid on its surface.

1.4 Present research

Over the past decade, there is a strong interest to understand DNA condensation with multivalent counterions. This is because its logical relation between gene therapy and the need of developing specialized disease-fighting treatments. Any human gene therapy product for sale has not been approved yet by the Food and Drug Administration [38]. The current gene therapy is in the experimental stage and not proved to be very successful in clinical trials [38]. In order to develop a successful and effective way of gene therapy, it is necessary to completely understand the DNA behavior in salt solution, its condensation and packed process, its stable condensed morphology, its elastic behavior under multivalent counterions, and its release process. Electrolyte solutions can be well described by the linearized Poisson-Boltzmann (PB) or the so called Debye-Hückel equation, however this approximation is no longer valid for polyelectrolytes such as DNA molecules [40]. Theoretical approaches, including the Poisson-Boltzmann (PB) theory [41] and the counterion condensation theory of Manning [42, 43], deal with solutions of monovalent ions and primitive model of the DNA. In these theories, the ions are treated as charged spheres and the DNA is treated as a hard uniformly charged cylinder, embedded in a continuum dielectric. Computer simulations have shown that the PB equation provides a more solid basis for studying polyelectrolytes than approaches based on Manning condensation theory [44, 40]. Moreover, the results of simulations have shown that the Poisson-Boltzmann equation generally satisfactorily describes the properties of the DNA in monovalent ionic environment. However for multivalent ions, it noticeably underestimates the ion density close to the surface of DNA molecule. It was demonstrated in simulations that bead-spring chains can reproduce the behavior of polyelectrolytes [45, 46, 47, 48, 49]. Simulations of flexible polyelectrolytes in the absence of salt [50, 51] and in the presence of different condensing agents [52, 53, 54, 55] have been performed focusing on

different properties of polyelectrolytes. It was shown that a polyelectrolyte can be condensed into a toroid-like structure [56, 57] upon addition of trivalent or tetravalent counterions. The stiffness and the length of a polyelectrolyte is important for the toroidal formation. If the stiffness is high and the chain length is long, the polyelectrolyte would condense into toroid, otherwise, it would form a different structure such as a rod or sphere [56, 21]. The morphology of a single condensed DNA has been studied [21, 28, 58, 59], the stable structure is determined by the surface energy and it was found to be a toroid under poor solvent conditions. The elastic properties of a condensed DNA molecule have been investigated by many research groups using single-molecule techniques. The methods include magnetic tweezers [60] (range 0.01 to 10 pN), optical tweezers [61] (range 0.1 to 100 pN), AFM [62] (range 10 to 10,000 pN), etc. The advantage of using single-molecule techniques is, for example, that the force required to collapse the DNA molecule can be directly quantified from the measurements. The elastic behavior of DNA molecule is entropic in origin [63] and the worm-like chain (WLC) model basically can explain this entropic behavior. Comparisons of the predictions of the entropic theory are limited only to the low-force regime [64], where this theory is most applicable. A simulation was performed to stretched a polyelectrolyte in monovalent salt solution [65], in which the electrostatic properties and the scaling laws were studied. New features of a single condensed DNA molecule was found by using single-molecule techniques [5, 6, 7]. The FECs showed a “plateau force” and “stick-release pattern” behavior, which are different from the WLC model. To explain the “force-plateau”, an analytical calculation was done by Zhang et al.[66]. They proposed a formula which can estimate the force needed to decondensate a DNA molecule, this approximation was based on the reentrant condensation theory proposed by Nguyen et al. [14]. In order to explain the different FECs found in the experiments [5, 6, 7], Wada et al. [8] presented a phenomenological

model which describes these elastic responses of a collapsed DNA, their theory is based on the WLC model. Furthermore, Wada et al. [11] performed a Brownian dynamics of stretching a single condensed polyelectrolyte to investigate in detail this process. They found that the counterions in the “force-plateau” case behave differently from the counterions in the “stick release” case. For a “force-plateau” case, the condensed counterions are in a fluid phase with moderate correlations; however in the “stick release” case, the complex (DNA and its condensed counterions) possesses a short-range ionic crystal-like order with strong correlations. In addition, They found that the pulling velocity has a strong effect on the FEC, the higher the pulling velocity, the more perturbed the FECs are. Very recently, Ritort et al. [67] have experimentally investigated the transition of a condensed DNA molecule, when it is stretched. They have used polyaminoamide dendrimers to condense the DNA molecule and optical tweezers to stretch it out. They found that the complex (DNA-dendrimers) shows some similarities to chromatin in folding and refolding and the compaction ratios are basically the same. Although their results provide new informations about the DNA complexation, their study is only in the “plateau force” range. In spite of all the information about DNA condensation and its stretching process, it is not well understood yet what is the internal structure of the condensed DNA molecule, when the FEC shows the “plateau force” and “stick-release pattern”, and how its elastic behaviors is affected by the condensed counterions. It is worth mentioning that there is relatively few numerical works performed in the issue of stretching a condensed polyelectrolyte, because this problem is a nonlinear process which involves combined effects coming from the long-range Coulomb and nonequilibrium effects of the pulling velocity.

Chapter 2

Simulation Method and Setup

To simulate a long DNA is very complicated, if all the degrees of freedom of this long molecule and the interactions of its chemically realistic united atoms are taken into account. DNA molecule is a dense polyelectrolyte chain; therefore, it is required to construct a model similar to, but smaller in degrees of freedom than the real one, in order to reduce the complexity to make the simulation a tractable approach. The reduction of the degrees of freedom is called coarse graining. The coarse-graining approach is used to map larger units of the real DNA molecule onto one unit of a new chain. The interactions between the new units should reflect and mimic those of the chemically realistic chain. In this chapter, we will briefly review the DNA structure. A coarse-grained model of DNA will be explained. The atom sizes and which atoms take part in one new unit will be described. And finally, the molecular dynamic methodology will be introduced.

2.1 DNA structure

DNA is a long polyelectrolyte chain of small compounds called nucleotides which bear a charge of $-e$. These nucleotides are the basic building blocks of DNA, each

of which contains a sugar, a base and a phosphate group. The chain is formed by linking the sugars to one another through their phosphate group and it can be long as several *cm*. Watson and Crick [2] formulated a series of rules in order to explain how the building blocks form the DNA molecule (see figure 2-1). They based their assumptions on the information found in X-ray crystallography of DNA (Rosalind Franklin [68]) and the Chargaff rules [69, 70, 71, 72, 73, 74], which states that in any DNA, the concentrations of adenine equals thymine and guanine equals cytosine. Watson and Crick rules are summarized as follow

1. Two sets of base pairs are arranged in a double helix.
2. Phosphates and the sugar deoxyribose are arranged as a backbone with the carbon of one sugar linked through a phosphodiester to the carbon of the next sugar.
3. The bases are like rungs of a ladder, with adenine hydrogen bonded to thymine and guanine to cytosine.
4. The monomer spacing is 0.34 nm and the helical spacing is 3.4 nm per turn. Thus, one turn has 10 base pairs.
5. The two DNA strands, which make the double helix, are antiparallel.

Another feature of the double helix is that the strands are held together only by hydrogen bonds and by hydrophobic interactions between the bases. As a result, if these weak interactions are disrupted by heat, acidic or basic conditions, or chaotropic agents, the DNA strands can be separated. This separation is referred to as DNA melting or denaturation. The denaturation conditions are dependent on the proportion of AT and GC base pairs, and on the sequence of the bases. In general, DNA containing a higher proportion of GC bp is more stable, and DNA sequence with the repeated sequence “AT” is the least stable. The most important

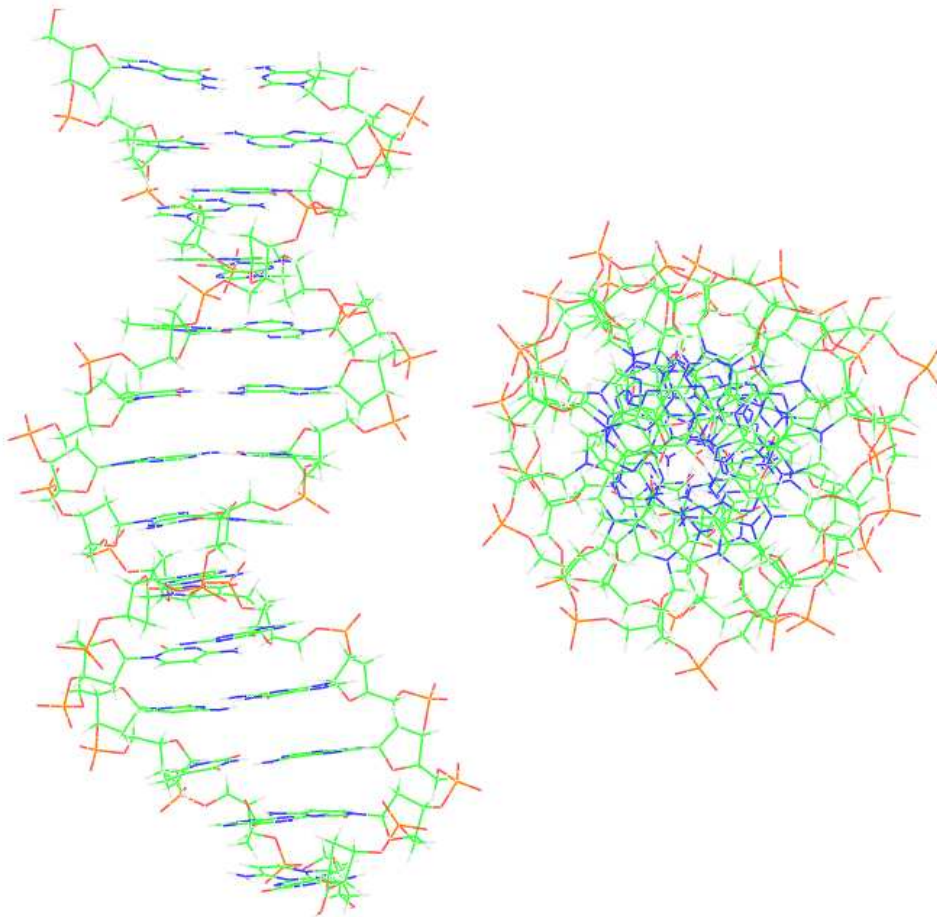


Figure 2-1: DNA structure illustrated by a right handed double helix, with about 10 nucleotide pairs per helical turn. Each spiral strand, composed of a sugar phosphate backbone and attached bases, is connected to a complementary strand by hydrogen bonding between paired bases, adenine (A) with thymine (T) and guanine (G) with cytosine (C). This structure was first described by James Watson and Francis Crick in 1953.

feature of the double helix regarding its function is that all the information in it is redundant. For example if one base is lost, the complementary base on the opposite strand still contains the information. This is the basis of one strand DNA repair. In this process, a damaged or missing base is replaced using the information on the opposite strand.

2.2 Coarse-grained model

In this study, the DNA model of Stevens [56] is employed. The most important characteristic of his model is that it has the same linear density of a DNA molecule, $-2e/3.4\text{\AA}$. He mapped the highly repetitive double-stranded DNA molecule into a single chain, where the chain is constructed by joining, one by one, DNA monomers with springs of average length of b . Each DNA monomer represents a phosphate group, a base and a sugar (see Figure 2-2). The coarse-graining process of DNA molecule is shown in the Figure 2-2. The coarse-grained model of DNA molecule contains N_{DNA} monomers, each of which carries a negative unit charge, $-e$, and the radius of monomers is r_{DNA} . In order to condense the DNA chain, it is required to add condensing agents to the system, as it is done in experiments. Spermine (SP) is chosen as condensing agent in this simulation. Spermidine is a small flexible polycation with a charge of $+4e$ and a length of 20\AA . In this study, spermine is mapped into one sphere bead, which has a radius r_{SP} and charge of Z_{SP} . The coarse-graining process of spermine is shown in the Figure 2-2. The Figure 2-3 shows a short DNA molecule and its counterpart the coarse grained model of the short DNA molecule.

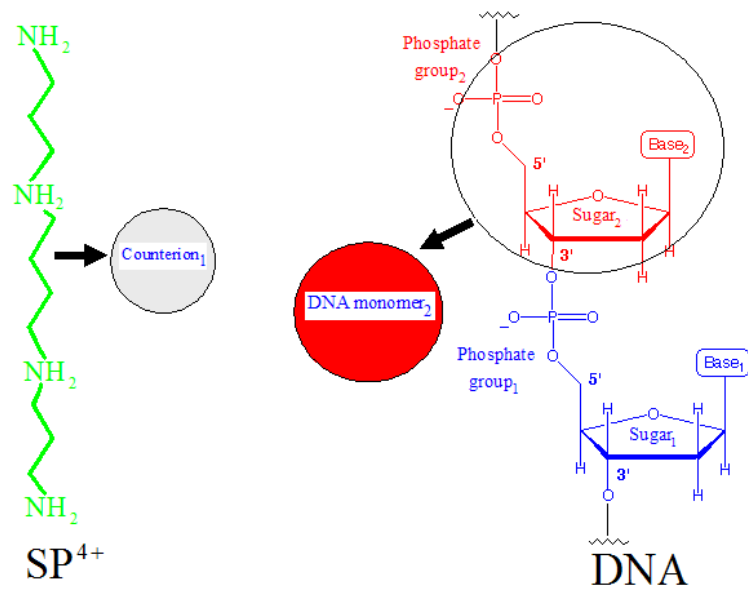


Figure 2-2: How to coarse grain a DNA molecule and its counterion. In our model, one DNA monomer represents one nucleotide (a phosphate with $-e$, a sugar and a sugar). Spermine is represented with one sphere.

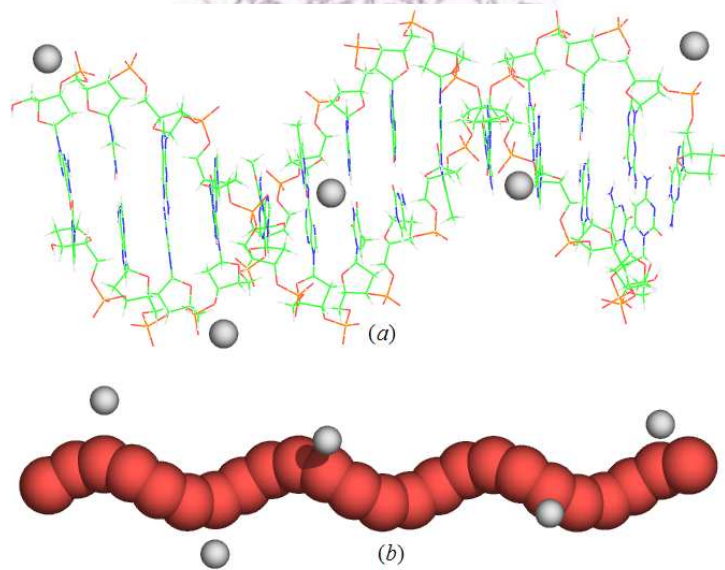


Figure 2-3: DNA molecule and its coarse grained model. a) A short DNA molecule represented with an atomistic model. Here all atoms are included. b) A coarse grained model of the DNA molecule. The red chain represents a dsDNA and the white spheres are meant to be its counterions

2.3 Molecular dynamics

Molecular dynamics simulation is performed and the temperature, T , is controlled by velocity Langevin thermostat. Molecular dynamics with the Langevin thermostat becomes a stochastic differential equation in which two additional force terms are being added to the equation of motion. The effects of solvent molecules are approximated by these two terms. The first term represents a frictional force which takes into account the frictional drag on the solute and the second one corresponds to random kicks associated with the thermal motions of the solvent molecules, $\vec{\eta}_i$. It is assumed that friction force is proportional to the particle's velocity and opposite to the direction of the particle motion. The equation of motion is therefore written as

$$m_i \frac{d^2 \vec{r}_i}{dt^2} = -m_i \zeta \frac{d\vec{r}_i}{dt} - \frac{\partial U}{\partial \vec{r}_i} + \vec{\eta}_i \quad (2.1)$$

where ζ is the damping constant, U is the total potential energy, and $\vec{\eta}_i$ is the vectorial random force acting on the particle i , which satisfies the fluctuation-dissipation theorem

$$\begin{aligned} \langle \vec{\eta}_i \rangle &= \vec{0} \\ \langle \vec{\eta}_i \cdot \vec{\eta}_j \rangle &= 6k_B T \zeta \delta_{ij} \delta(t - t') \end{aligned} \quad (2.2)$$

where δ_{ij} and $\delta(t-t')$ are the Kronecker delta and Dirac delta function, respectively.

The total energy for the system is the summation of the following terms

$$U = U_{LJ} + U_{ee} + U_r + U_\theta \quad (2.3)$$

where U_{LJ} is the Lennard-Jones potential, U_{ee} is the Coulomb potential, U_r is the harmonic potential and U_θ is the bond-angle potential. These potentials are explained in the following sections.

2.4 Force fields

The force fields refer to the interactions that one particle exerts on another particle or a collection of other particles. Generally speaking, the force field can be divided in two categories, a bonded and non-bonded interaction. In this study, bonded interactions act between particles which have a common bond or bond-angle, and they are divided into bond potential and bond-angle potential. They are calculated on the basis of a fixed list. Non-bonded interactions act between atoms in the same molecule and those outside the molecule. In this study, non-bonded interactions are separated into Coulomb interaction and excluded-volume interaction. They are computed on the basis of a neighbor list.

2.4.1 Non-bonded interactions

Excluded-volume potential

The excluded volumes of particles, including the monomers and the counterions, are described by Lennard-Jones (LJ) potential, which is represented by an attractive and a repulsive term. The attractive term represents the van der Waals interaction due to induced dipole-dipole interaction. The repulsive term arises from the nonbonded overlap between electron clouds and has an arbitrary form. The LJ potential repels at close range, then attracts, and at long range vanishes. It is defined by

$$U_{LJ}^{ij}(r_{ij}) = 4\varepsilon_{LJ} \left[\left(\frac{\sigma_{ij}}{r_{ij}} \right)^{12} - \left(\frac{\sigma_{ij}}{r_{ij}} \right)^6 \right] \quad (2.4)$$

where r_{ij} is the separation distance between particle i and j , ε_{LJ} is the strength of LJ interaction, which describes the hardness of explicit particles, and σ_{ij} is the collision diameter. The Lorentz-Berthelot mixing rule is applied for the interaction between different kinds of particle, $\sigma_{ij} = (\sigma_{ii} + \sigma_{jj})/2$. Since water is a good solvent

for DNA molecule, the LJ interaction is cutoff at $r_c = \sqrt[6]{2}\sigma_{ij}$ in this study and shifted to $-U_{LJ}^{ij}(r_c)$, which yields a purely repulsive shifted-truncated LJ potential. The modified Eq. 2.4 can be written as

$$U_{LJ}^{ij}(r_{ij}) = \begin{cases} 4\varepsilon_{LJ} \left[\left(\frac{\sigma_{ij}}{r_{ij}} \right)^{12} - \left(\frac{\sigma_{ij}}{r_{ij}} \right)^6 \right] + \varepsilon_{LJ} & \text{for } r_{ij} \leq r_c, \\ 0 & \text{for } r_{ij} > r_c \end{cases} \quad (2.5)$$

Coulomb potential

The particles also interact with each other via electrostatic interaction. The electrostatic interaction is defined by the Coulomb's law, which states that the magnitude of the electrostatic force between two point charges is directly proportional to the magnitudes of each charge and inversely proportional to the square of the distance between the charges. The Coulomb potential is thus written as

$$U_{ee}^{ij}(r_{ij}) = k_B T \lambda_B \frac{Z_i Z_j}{r_{ij}} \quad (2.6)$$

Here Z_i , Z_j are the valances of particles i and j , respectively, k_B is the Boltzmann constant, and λ_B is the Bjerrum length defined as the distance at which the Coulomb potential of two unit charges e is equal to the thermal energy $k_B T$. λ_B can be expressed as $e^2/(4\pi\epsilon_o\epsilon)k_B T$ where ϵ is the dielectric constant of the continuum and ϵ_o is the vacuum permittivity.

Particle-particle particle-mesh (PPPM) algorithm is used to calculate the long-range Coulomb interaction, in which interactions with periodic images are taken into account. The PPPM method, which is an alternative approach to the Ewald sum and was proposed by Hockney and Eastwood [75], is an accurate and computationally efficient method for calculating interactions in molecular simulations. The PPPM method is based on separating the long-range inter-particle force into the sum of rapidly-varying short-range interactions and slowly-varying long-range

interactions. The PPPM method is computed by two steps, first, by a PP method, and then by a PM method. The PP method is used to find the total short-range contribution to the force on each particle and is only computed by direct particle-particle summation within some cutoff radius. Then, the PM method is used to compute the total slowly-varying long-range interaction contributions which is calculated in the reciprocal space, approximated on a grid.

2.4.2 Bonded interactions

Harmonic potential

Neighboring DNA monomers on the chain are connected by a spring, described by a harmonic potential. The harmonic potential, associated with small bond stretches about the equilibrium bond length, can be approximated by a parabolic equation, and it is defined by

$$U_r^{ij}(r_{ij}) = k(r_{ij} - b_o)^2 \quad (2.7)$$

where k is the spring constant that gives the stiffness of the bond and b_o is the equilibrium distance.

Bond-angle potential

The DNA chain is given an intrinsic stiffness by including a bond-angle potential. It is modeled by a three-body potential acting among adjacent bead triplets on the chain, and it is defined by

$$U_\theta^{ijk}(\theta_{ijk}) = k_1(\theta_{ijk} - \theta_o)^2 + k_2(\theta_{ijk} - \theta_o)^4 \quad (2.8)$$

where θ_{ijk} is the bond angle between three consecutive beads, $(i, j, k = i-1, i, i+1)$, and θ_o is the equilibrium angle, whose value is π rad. k_1 and k_2 are spring constants.

2.5 Integration algorithm

In this study, the velocity-Verlet algorithm is used to integrate the equation of motion. There are various versions of Verlet algorithm and even new numerical integration schemes. However, the velocity-Verlet algorithm is, at the same time, simple, accurate and stable. The velocity-Verlet algorithm generates a phase-space trajectory which is a sequence of “snapshots” for the particle coordinates and velocities at time t , by the following procedure

$$\begin{aligned}\vec{r}(t + d\tau) &= \vec{r}(t) + \vec{v}(t)d\tau + \frac{1}{2}d\tau^2 \frac{\vec{f}(t)}{m} \\ \vec{v}(t + d\tau) &= \vec{v}(t) + \frac{\vec{f}(t) + \vec{f}(t+d\tau)}{2m} d\tau,\end{aligned}\tag{2.9}$$

where $d\tau$ is a small time increment and $\vec{f}(t)$ is the total force acting on a particle at time t . If the initial conditions $\vec{r}(0)$ and $\vec{v}(0)$ are given, it is possible to compute $\vec{v}(t)$ and $\vec{r}(t)$, sequentially by applying Equations 2.9.

2.6 Simulation setup

In the present work, the morphology of a condensed DNA molecule and its stretching process are studied by molecular dynamics simulation. In a real system, where a single DNA molecule is stretched, is composed of a DNA molecule, which contains N_{DNA} negatively charged monomers of valence $Z_{DNA} = -1$, N_{DNA} monovalent counterions dissociated from the DNA, N_c multivalent ($Z_c : 1$) salts, which dissociate into N_c multivalent counterions of valence Z_c and $Z_c N_c$ monovalent coions, and N_m monovalent (1:1) salts, which dissociate into N_m monovalent counterions

and N_m monovalent ions. To simplify the real system and make our simulation a tractable approach, we consider that our system is composed of one DNA, which contains N_{DNA} negatively charged monomers, we neglect the dissociated counterions coming from the DNA and multivalent salts because their influence is not too strong to modify the elastic behavior of the DNA [64]. Moreover, we reduce the number of particles coming from the monovalent salts by assuming that they dissociate only into N_m negatively charge particles, when the total charge of the multivalent counterions is larger than the DNA charge, or N_m positively charge particles, when the DNA charge is larger than the total charge of the multivalent counterion, and their amount is equal to the number of required particles which keep the overall system neutral. Our system is placed in an aqueous solution at room temperature. The temperature, $T = 1.2\varepsilon_{LJ}/K_B$, is controlled by using the Langevin thermostat with damping constant ζ and time step dt equal to $1/\tau$ and 0.015τ , respectively, where τ is the LJ time unit, $\tau = \sigma\sqrt{m/\varepsilon_{LJ}}$. The simulation box is rectangular whose volume is V . Periodic boundary conditions are applied in all the directions of this simulation box. The radius of the DNA chain, r_{DNA} , and the counterion, r_c , are varied in this simulation. It is assumed that the mass of the particles, including DNA monomers and all kind of ions, have the same value m . The DNA concentration is fixed at $2.8210^{-5}\sigma^{-3}$. The solvent is treated at the primitive level and the Bjerrum length, which describes the strength of Coulomb interaction, is set to $\lambda_B = 4.73\sigma \approx 7.1 \text{ nm}$. This value mimics an aqueous environment at room temperature. The non-bonded interactions are neglected for atoms sharing a common bond or bond angle, as well as up to the 1-4 interactions. The particle-particle particle-mesh (PPPM) algorithm is used to calculate the long-range Coulomb interaction. the strength of LJ interaction, ε_{LJ} is set to be $1.2k_B T$. The parameters of the bond potential are chosen as $k = 100K_B T/\sigma$ and $b_0 = 1.1\sigma$. The parameters of the bond-angle potential are

set to be $k_1 = 5K_B T / rad^2$, $k_2 = 20K_B T / rad^2$ and $\theta_o = \pi rad$. The velocity-Verlet algorithm is applied to integrate the equation of motion (Eq. 2.1). Similar work has been performed by Stevens [56] and the results showed that DNA is highly organized in the presence of multivalent counterions. Following his work, a spiral structure is chosen as the initial configuration of our DNA chain. Then, the DNA chain is collapsed into a toroid-like structure after reaching equilibrium state by the condensed tetravalent counterions. In this process, each simulation takes around 10^7 time steps to reach the equilibrium state, then the system is required to equilibrate for 5×10^7 time steps in which data are collected every 1000 steps. In addition, the properties of the system are computed by using standard statistic method. To stretch the DNA molecule, one configuration of the condensed DNA toroid in the equilibrium state is chosen as an initial configuration for the stretching process. Then, the single condensed DNA molecule is stretched by fixing the position of one end and pulling the other end at a constant velocity. Because the pulling velocity is relatively high, the force profile contains both force data and noise. A low-pass filter is used to separate the force data and the noise. “The Nyquist-Shannon sampling theorem” [76] is employed to filter the data to avoid unphysical results. This theorem states that exact reconstruction of a continuous-time baseband signal from its samples is possible if the signal is band limited and the sampling frequency is greater than twice the signal bandwidth, which means that if it is known that a signal has a certain highest frequency, f_B , then the theorem gives a lower bound on the sampling frequency, f_s , to allow perfect reconstruction of the sampled signal. This lower bound to the sampling frequency is equal to $2f_B$ and called the Nyquist rate. Therefore, this theorem is written as

$$2f_B < f_s \tag{2.10}$$

Chapter 3

Results and Discussions

In this chapter, we show and discuss our results. This chapter is divided into two parts. First, we discuss the static properties of the condensed DNA molecule, (shape, size, etc.). Then, we discuss the response of the system to an external applied force and show how the contribution of the condensed counterions affects the behavior of the DNA molecule.

3.1 Toroidal structure of a single condensed DNA molecule

Experiments and simulations confirmed that a DNA molecule can be condensed into a toroidal structure [28, 30, 32, 33, 34, 35, 36, 56, 57] and the toroid has a characteristic size, which is in the order of its persistence length. In this section, the size and shape of a condensed DNA molecule are characterized.

If the condensed DNA molecule displays a toroidal shape, a major radius, R , and a minor radius, r_o , can be defined as shown in Figure 3-1(a). The position of each particle, which forms the toroid (DNA plus condensed counterions), can be

described by the following toroidal coordinates

$$r_x = [R + r_o \cos v] \cos u, \quad r_y = [R + r_o \cos v] \sin u, \quad r_z = r_o \sin v \quad (3.1)$$

where the major radius, R , is the distance from the center of the tube to the center of the torus, the minor radius, r_o , is the radius of the tube, and u, v are angles in the interval $[0, 2\pi)$ (See Figure 3-1(b)). The volume of this toroid can be expressed as a function of R and r_o , and is equal to

$$V = (\pi r_o^2) (2\pi R) = 2\pi^2 R r_o^2 \quad (3.2)$$

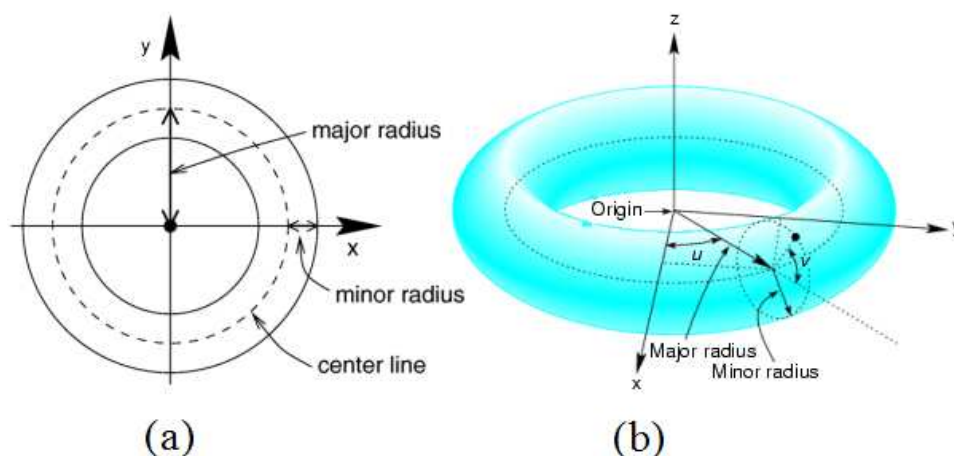


Figure 3-1: Characteristic parameters of a toroid (a) in 2D projection and (b) in 3D. The major radius, R , and the minor radius, r_o , are shown in (a) and (b). Figure (b) shows also the angles u and v for Eq. 3.1.

3.1.1 Gyration tensor

A fundamental way to study the shape of a polymer is to investigate the gyration tensor of the polymer, which describes the second moments of position of a collection of particles, and can be defined as

$$T_{\alpha\beta} = \int_V dr^3 \frac{n(r)}{V} r_\alpha r_\beta \quad (3.3)$$

where $n(r)$ is the number of particles at position \vec{r} in the frame of the center of mass. $\alpha, \beta = x, y, z$ denote the three Cartesian components. It is possible to calculate the principal moments of $T_{\alpha\beta}$ as a function of the major and minor radii of the toroid. That can be done by replacing Eq. 3.1 and Eq. 3.2 in Eq. 3.3 and integrate it. Consider that λ_1, λ_2 and λ_3 are the three principal moments of $T_{\alpha\beta}$. Then, λ_1, λ_2 and λ_3 can be shown to read as

$$\lambda_1 = \frac{r_o^2}{4}, \quad \lambda_2 = \frac{(4R^2 + 3r_o^2)}{8}, \quad \lambda_3 = \frac{(4R^2 + 3r_o^2)}{8}, \quad (3.4)$$

Two of these moments are equal ($\lambda_2 = \lambda_3$) and their values are larger than the third value (λ_1). This is always true for a perfect toroid.

3.1.2 Asphericity

Asphericity is a quantity that is used to quantify the shape of a macromolecule. This quantity measures the deformation from a spherical geometry and it takes a value between 0 (sphere) and 1 (rod) and is defined as

$$As = \frac{1}{2} \left\langle \frac{(\lambda_1 - \lambda_2)^2 + (\lambda_2 - \lambda_3)^2 + (\lambda_3 - \lambda_1)^2}{(\lambda_1 + \lambda_2 + \lambda_3)^2} \right\rangle \quad (3.5)$$

Replacing Eq. 3.4 in Eq. 3.5 gives the asphericity for a perfect toroid as

$$A_s = \frac{1}{64} \left[1 + \frac{3}{\left[1 + \left(\frac{r_o}{R} \right)^2 \right]} \right]^2 \quad (3.6)$$

In Eq. 3.6, we see that the asphericity depends on the ratio of r_o/R . For $r_o/R \approx 0$, the value of A_s goes to 0.25, which corresponds to the asphericity of a ring. It is important to be aware that for a toroid, the value of r_o/R is not zero; however this ratio is small.

In a real case, DNA does not form a perfect toroid. The values of λ_2 and λ_3 are a little bit different in their values but very close to each other, ($\lambda_3 \approx \lambda_2 > \lambda_1$). Assume that r_o is a constant and the difference between λ_2 and λ_3 are mainly due to the variation in R , which means that λ_2 and λ_3 have a specific R_1 and R_2 , respectively. It modifies Eq. 3.4 to

$$\lambda_1 = \frac{r_o^2}{4}, \quad \lambda_2 = \frac{(4R_1^2 + 3r_o^2)}{8}, \quad \lambda_3 = \frac{(4R_2^2 + 3r_o^2)}{8}, \quad (3.7)$$

First, the principle moments of the condensed DNA molecule are calculated by using Eq 3.8, and then R_1 , R_2 and r_o are estimated by applying the approximation given in Eq 3.7. In Eq. 3.6, R is assumed to be $(R_1 + R_2)/2$. These analytical results, Eq. 3.6 and Eq. 3.7, will be used in the following sections to analyze the results obtained from our simulations.

3.2 Counterion size

It is known that spermine is protonated to interact with the negative charges along DNA and it can help DNA molecule to pack nicely. In Chapter 2, a coarse grained model for DNA and its counterions was introduced. Here, this coarse

Table 3.1: DNA monomer and counterion diameter.

Case	I	II	III	IV	V	VI	VII
DNA	σ	2σ	2σ	2σ	2.6σ	3σ	3.5σ
SP	σ	2σ	σ	0.5σ	0.6σ	σ	0.5σ

grained model is employed to perform the simulation. It has been shown that the counterion size is an important factor to determine the behavior and the properties of a polyelectrolyte [54]. Therefore, instead of arbitrarily choosing a diameter for our DNA monomer and its counterion, simulations are performed to study the influence of the counterion size and DNA monomer size on the final conformation of DNA molecule. The asphericity, which is 0.25 for a ring, is used as a criterion to judge whether or not the system has formed a toroidal structure in which it should be close to 0.25 for small r_o/R . It is known that the ionic sizes of particles are usually in the range 1\AA to 3\AA [77, 78, 79]. Thus, the ionic size of the counterion and DNA monomer are systematically varied in this range, as shown in the table 3.1. In our study, σ corresponds to 1.5\AA . The initial configuration of the system is given as a spiral structure [56]. In this part of study, the system is composed of one DNA of chain length $N_{DNA} = 256$ and 64 tetravalent counterions ($N_{SP} = 64$).

The asphericity is calculated by using Eq. 3.5 and the results are plotted in the figure 3-2. Because the asphericity curves carry high frequency noise that makes difficult to analyze it, a low-pass filter is applied to reduce the noise and smooth the curves which are shown in Figure 3-3. Figure 3-3 shows that the asphericity in sets I,III,IV,V are more stable than set II and VI because their amplitude fluctuations are small and they oscillate around a fixed value. This fluctuation can be understood by noticing that if the ratio (r_o/R) in Eq. 3.6 is not kept constant through the time, the asphericity would oscillate. In set II

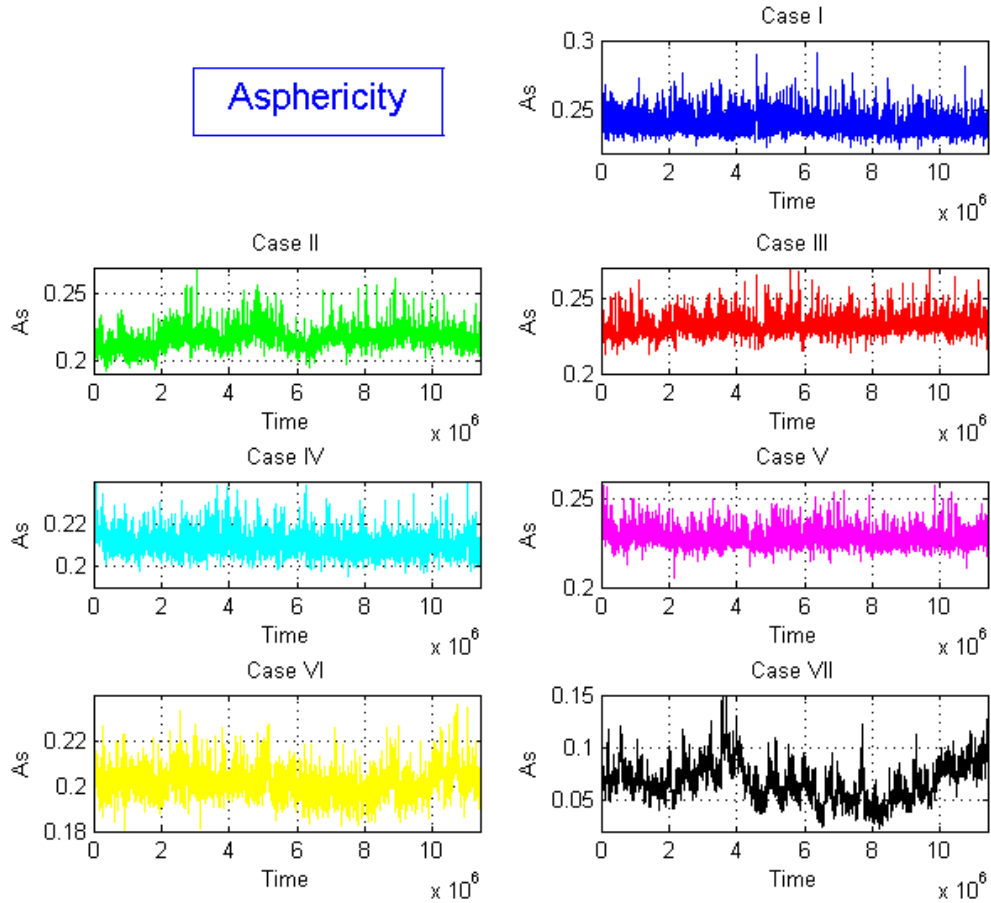


Figure 3-2: Asphericity plotted for each case in the table 3.1 before filtering the noise.

and VI, DNA chains form an unstable toroid because the ratio (r_o/R) changes faster than the others cases mention above. On the other hand, set I,III,IV and V are stable because this ratio is almost constant, which means that the DNA, most of the time, maintains a toroid-like structure. A ring would be formed if

the ratio (r_o/R) is equal to 0, in this condition the asphericity will be 0.25. It is observed in the same figure that the relation between asphericity for these cases are $As(I) > As(III) > As(V) > As(IV)$. Furthermore, the set I and III are closer to the value of 0.25 which means that the ratio (r_o/R) is very small. In set VII, DNA chain can not form a toroid because its asphericity is much smaller than 0.25. It is known that the electrostatic interaction between the DNA and the polyamine is via the oxygen, which belongs to the phosphate group on the DNA backbone, and the nitrogen, which is the protonated particle in the polyamine. The effective ionic radius for oxygen is larger than that for nitrogen. Thus, the set III is adopted as the size of our system through this study because this set gives a larger ionic radius for the DNA monomer and a smaller radius for the counterion, which mimics the real system, and produces a stable toroid as well.

3.3 Size and shape of a condensed DNA molecule

In the preview section a DNA chain was condensed into a toroid-like structure in the presence of tetravalent counterions. In this section, the initial configuration dependence of the DNA chain over its final conformation (r_o, R_1, R_2, As) is analyzed.

3.3.1 Gyration tensor

In the previous section the gyration tensor's equation was introduced in the continuum space. Here, this equation is modified to a discrete space since our systems is made of discrete spherical particles. The discretization of Eq. 3.3 can be written as

$$T_{\alpha\beta} = \frac{1}{N} \sum_{i=1}^N (\vec{r}_\alpha^{(i)} - \vec{r}_{cm})(\vec{r}_\beta^{(i)} - \vec{r}_{cm}) \quad (3.8)$$

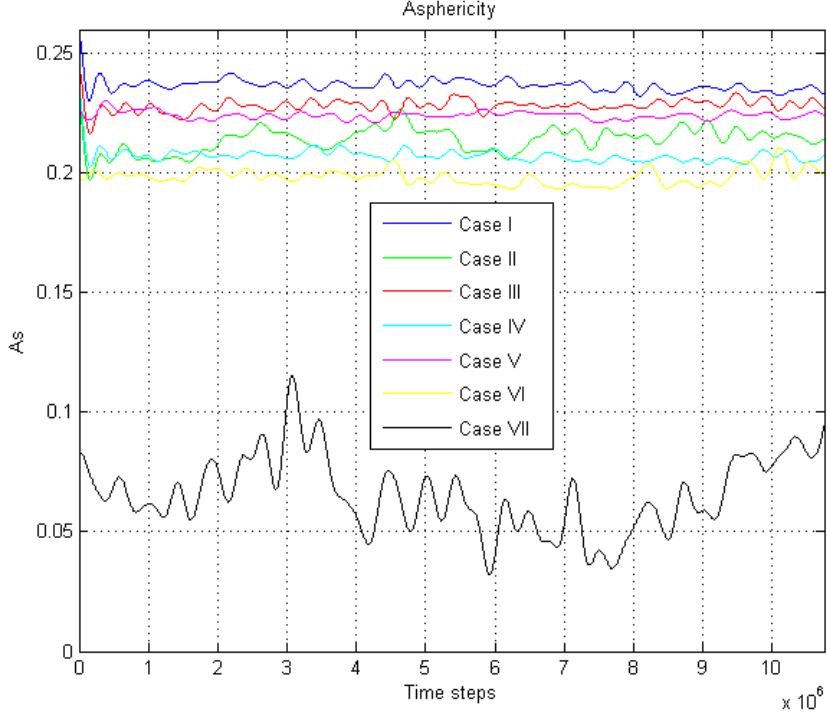


Figure 3-3: Asphericity illustrated for the cases in the table 3.1

where $\vec{r}^{(i)}$ is the position vector of the i^{th} particle. $\alpha, \beta = 1, 2, 3$ denote the three Cartesian components and \vec{r}_{cm} is the position of the center of mass of the polyelectrolyte. The simulations are started with different initial spiral radii to see whether the radii can have influence in the final conformation or not. For example, different radius could produce different toroid size, or even, different condensed structure. The system is composed of one DNA chain ($N_{DNA} = 256$) and tetravalent counterions ($N_{SP} = 64$). The principle moments of the complex are calculated by applying Eq 3.8. Then, R_1, R_2 and r_o are estimated by using the

approximation given in Eq 3.7. It is found that the condensed DNA toroid has different values of R_1 and R_2 (as mentioned in subsection 3.1.2); however, they are very close in their values to each other, ($R_1/R_2 \approx 1.115$), see Figure 3-4. This is because the complex (DNA molecule plus condensed counterions) is in dynamic equilibrium, and the tetravalent counterions are not bound on a fixed position of the DNA chain, instead they are in a dynamic motion trapped in a condensate tube. The motion of the condensed DNA toroid and the motion of the counterions inside the tube perturb the complex and therefore do not allow them to form a perfect toroid. In the same figure, it is observed that r_o is almost constant. Therefore, after the system reaches the equilibrium state, the final conformation is not dependent of the initial configuration, as shown in Figure 3-4. Moreover, the final conformation is basically identical although the spiral radius of each initial configuration are different. It can be seen that their asphericities are close to 0.25, as shown in Figure 3-6, which means that the DNA maintains a toroid-like structure after reaching the equilibrium state (See Figure 3-5).

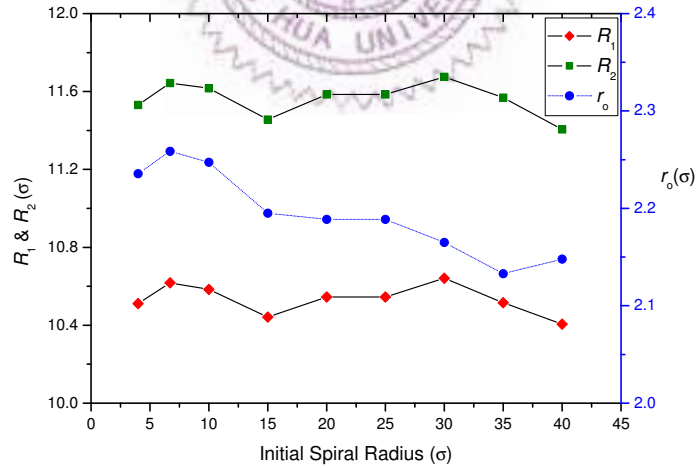


Figure 3-4: Final values of R_1 , R_2 and r_0 as a function of the initial spiral radius.

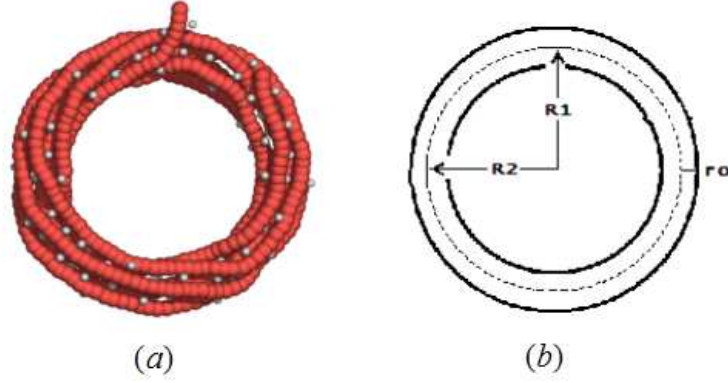


Figure 3-5: (a) Snapshot of a DNA in the equilibrium state (parameters of case III, table 3.1). The red chain represents the dsDNA and the small white spheres represent the tetraivalent counterions. (b) Schematic illustration of a toroid. For a perfect toroid, the radii R_1 and R_2 are equal. r_o represents the minor radius. One can observe that these two Snapshot are identical.

3.3.2 The winding number

The winding number, $W(u)$, determines how many times a toroidal DNA winds around a specific axis. It is calculated by

$$W(u) = \frac{1}{2\pi} \oint_S d\theta = \frac{1}{2\pi} \int_{u=0}^{u=L} \theta(u) du \quad (3.9)$$

where $\theta(u)$ is a positive counterclockwise angle along the DNA chain. In our simulation, the winding number is calculated by defining the principal axis which passes through the center of the toroid and is perpendicular to the plane formed by the other two principal axes such as axis z in Figure 3-1. The angles, which forms the consecutive particles on the chain with the axis, are summed starting from the first DNA monomer and ending in the last DNA monomer. The winding number is then calculated by dividing this angle over 2π . In Figure 3-6, it is shown how $W(u)$ varies with initial spiral radius. It is observed that $W(u)$ does not depend significantly on the initial configuration. The winding number is a key quantity to

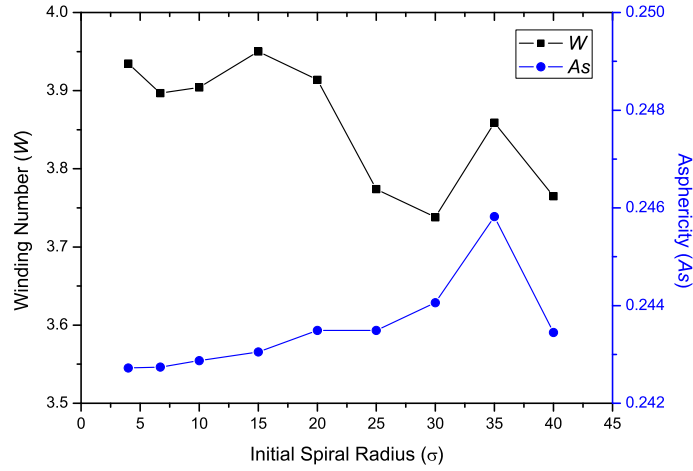


Figure 3-6: As and W as a function of the initial spiral radius. The value of the Asphericity is close to 0.25. This clearly shows that the DNA is toroid-like.

understand the evolution of the extension of the condensed DNA molecule during a stretching process.

3.4 Stretching process and pulling velocity

This section is to study the stretching process of a single condensed DNA molecule. In most experiments [5, 6, 7, 67] a single DNA molecule in dilute solution, where the DNA concentration and monovalent salt concentration were fixed, was condensed by increasing gradually the multivalent counterion concentration. After condensation, the condensed DNA molecule was stretched by using optical tweezer at different multivalent counterion concentration. The FEC were measured in this process by trapping one bead using a fixed laser beam and the other with a movable beam (These two beads were tethered to the free DNA ends). The extension of the single DNA molecule was determined by subtracting the bead's radii from the distance between the 2 bead centers and the force acting on the single DNA

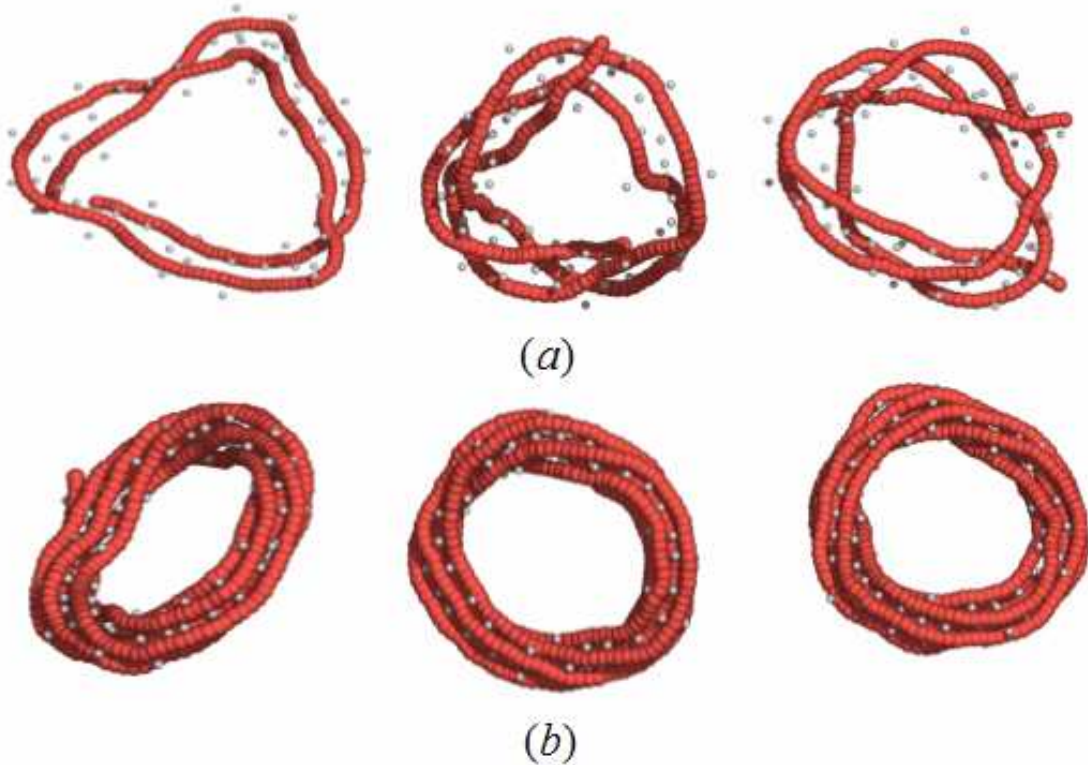


Figure 3-7: (a) Evolution of a DNA molecule during the simulation. The tetraivalent counterions (white sphere) tend to condense on the DNA in order to decrease the Manning constant [42]. (b) Condensed DNA toroid after reaching the equilibrium state. It can be seen that the DNA molecule forms a well-defined toroid-like structure. The two neutral chains are not shown for the clarity of the pictures.

molecule was determined from the displacement of the bead from the fixed beam spot. These experiments showed that the elastic response of a single condensed DNA molecule is different from the response of a single DNA molecule in the coil state. WLC behavior for $C < C_c$ (See appendix A), force plateaus for $C \sim C_c$ in which the FEC displayed a constant force in a wide range of the DNA's extension and its value depends strongly on the counterion concentration, and stick-release patterns for $C_c \ll C < C_d$ in which the FEC shows a repeatedly elastic response during stretching that can be described by a WLC at large extension. WLC re-

Table 3.2: Parameters of the condensed DNA toroid calculated at the equilibrium state. For $N_{DNA} = 512$ and $N_{SP} = 128$

Parameters	
$\langle r_o \rangle$	3.84σ
$\langle R_1 \rangle$	10.77σ
$\langle R_2 \rangle$	11.74σ
$\langle b \rangle$	1.0822σ
$\langle As \rangle$	0.2177
$\langle W \rangle$	7.5

curs for $C > C_d$, which suggests a reentrant condensation of the DNA at the single molecule level.

3.4.1 Stretching process

In our simulation, a DNA molecule of chain length $N_{DNA} = 512$ is collapsed into a toroid-like structure in the presence of $N_{SP} = 128$ tetravalent counterions. In order to avoid that our DNA chain forms knots in the condensation process, a small neutral chain, which is composed of 100 neutral atoms, is connected to each one of the free DNA ends. These neutral atoms have the same characteristic of the DNA monomers, and they are connected to each other and to the free DNA ends by a harmonic potential (with spring constant, $k = 100k_B T/\sigma$, and equilibrium distance $b_o = 1.1\sigma$). The new two ends of the system (DNA plus neutral chains) are put apart and kept fixed in position. Therefore, the DNA can not form a knot while it condenses into a toroidal structure. The system is then required to equilibrate for 5×10^7 times steps, see Figure 3-7. After the DNA condenses into toroid-like structure, its size and shape are measured as explained in the Section 3.3. Its parameters in the equilibrium state are as shown in the Table 3.2. It is worth to mention that this DNA is twice longer than DNA studied in the Section

3.3; however they have the same average of major radius. It agrees with the experimental result of Widom et al. [80] which argued that the dimension and morphology of a condensed DNA particles are largely independent of the length of the DNA. To stretch the condensed DNA molecule, one configuration of the condensed DNA toroid in the equilibrium state is chosen as an initial configuration for the stretching process. Starting from this configuration, the two small neutral chains are removed and two neutral faked atoms (blue sphere in Figure 3-8), which have the same characteristics as the DNA monomers, are connected to the two free DNA ends by springs described by a harmonic potential ($k = 100k_B T/\sigma$ and $b_o = 1.1\sigma$). MD simulation is performed to emulate the stretching process and measure the elastic response. Moreover, the chosen initial configuration is rotated in order that these two faked atoms lie on the x-axis of the simulation box, where x-axis is the pulling direction. One faked atom is kept fixed while the another is pulled at constant velocity. The pulling velocity is along the x-axis direction and its value is varied as shown in the table 3.3. The stretching force in this process is calculated by

$$F_x = -\frac{\partial U_r}{\partial x} = -2k \frac{\sqrt{(x_i - x_j)^2 + (y_i - y_j)^2 + (z_i - z_j)^2} - b_o}{\sqrt{(x_i - x_j)^2 + (y_i - y_j)^2 + (z_i - z_j)^2}} (x_i - x_j) \quad (3.10)$$

where i is the atom located at one DNA end and j is the faked atom joined to this DNA end. x, y, z represent the coordinate position of these atoms measured in the frame of the simulation box.

3.4.2 Pulling velocity

In the previous sections, we have prepared our DNA sample for the stretching process. However, there is still an important consideration that must be taken into account before going on stretching a DNA molecule. This is the pulling

Table 3.3: The pulling velocity expressed in σ/τ units.

Velocity	σ/τ
$V(I)$	5×10^{-4}
$V(II)$	1×10^{-3}
$V(III)$	5×10^{-3}
$V(IV)$	1×10^{-2}
$V(VI)$	5×10^{-2}
$V(VI)$	1×10^{-1}

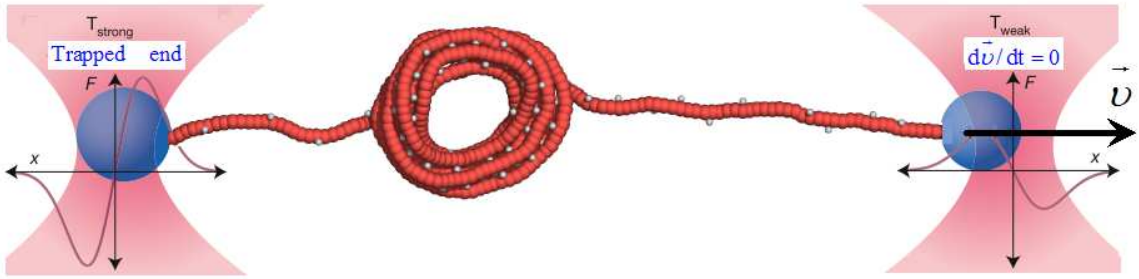


Figure 3-8: Snapshot of a single condensed DNA toroid being stretched. One end is fixed when the other is pulled at constant velocity. It is observed that the DNA is stretched one turn by one turn. Here, the size of the faked atoms (blue sphere) are enlarged to make a difference between the DNA monomers and the two faked atoms.

velocity. Here the effects of the pulling velocity on the FEC are studied. It is known that stretching a condensed polyelectrolyte is a non-equilibrium problem; therefore, the pulling velocity needs to be small enough to maintain the system in a “quasi-equilibrium” state. We assume that our polyelectrolyte has a relaxation time, τ_R , which can be described by the Rouse model. The Rouse relaxation time is the time required for the polymer’s center of mass to diffuse a distance, R_s , comparable to the size of the polymer ($R_s \approx R + r_o$). The Rouse model predicts the relaxation time as

$$\tau_R = \frac{\gamma b^2 N^2}{3\pi^2 k_B T} \quad (3.11)$$

where γ is the friction constant ($\gamma = m\zeta$), b is the bond length, and N is the number of monomers on the polymer. The average velocity for the polymer to diffuse a distance R_s is equal to

$$V_o = \frac{R_s}{\tau_R} = R_s \frac{3\pi^2 k_B T}{\gamma b^2 N^2} \quad (3.12)$$

In our case V_o is $\sim 1.68 \times 10^{-3} \sigma / \tau$ which corresponds to $\sim 3 \times 10^5 \mu m / s$ for a DNA in real units. This is a reference velocity because at velocities larger than this value the polyelectrolyte will not have time to relax. Moreover, this reference velocity is roughly 5 orders of magnitude larger than those applied in most experiments in which a DNA is pulled at much lower velocities whose values range from $0.15 \mu m / s$ to $2.12 \mu m / s$ [81]. However, we choose pulling velocities close to the reference value (see Table 3.3) which are several orders of magnitude larger than most experiments because with a pulling velocity in the same order of those experiments a typical simulation would take several months to stretch a small DNA chain. In order to study the influence of the pulling velocity over the FEC, the velocities are chosen smaller and larger than the reference value, V_o . In Table 3.3, we can see that the velocities (I) and (II) are smaller than the reference velocity but the velocity (III), (IV), (V), (VI) are larger than it. Due to the high pulling velocity, the force profile contains both wanted information, force data, and unwanted information, noise (See Figure 3-9). A low-pass filter is used to get rid of this noise. We mention that the noise in the force profile is dominant when the pulling velocity is high. All the curves in the following part of this section are plotted after the filter is applied. We calculate the force applied on the DNA molecule in both DNA ends. If the DNA is stretched in an “quasi-equilibrium” state, both force profiles should have the same response. Figure 3-10 is the response of the DNA monomer which is connected to the fake atom whose velocity is constant. We observe that the force curves

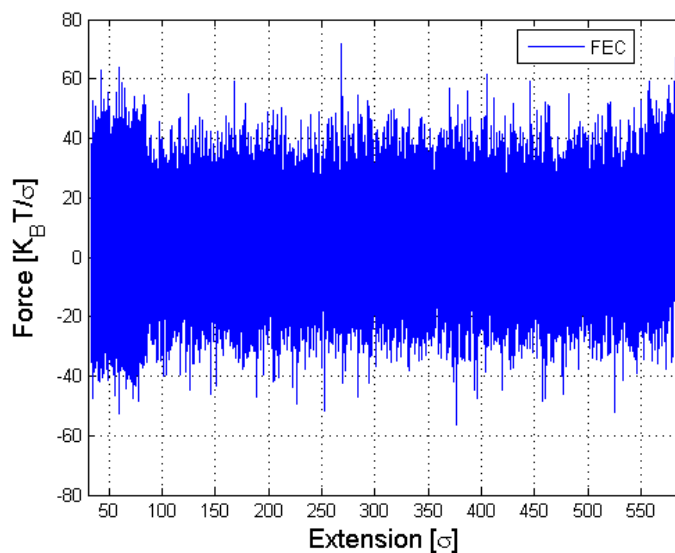


Figure 3-9: Force-extension curve (raw data) plotted with pulling velocity equals to $V(I) = 5 \times 10^{-4}$.

obtained with different pulling velocities $V(I), V(II), V(III), V(IV), V(V)$, and $V(VI)$ have different elastic responses. In the curves $V(I), V(II), V(III)$, and $V(IV)$, the oscillation becomes stronger as the pulling velocity is increased, which means that the complex has less time to relax when the velocity is risen to a high value. In curve $V(V)$ and $V(VI)$, the pulling velocity is so high that the condensed DNA chain experiences a rapidly transition between being condensed and becoming extended. In this process, the complex is forced to follow the direction of the pulling velocity and its natural behavior is changed. We find that as the pulling velocity increases, the force required to stretch the chain increases and the dependence of FEC over the pulling velocity is linear. Moreover, the higher the pulling

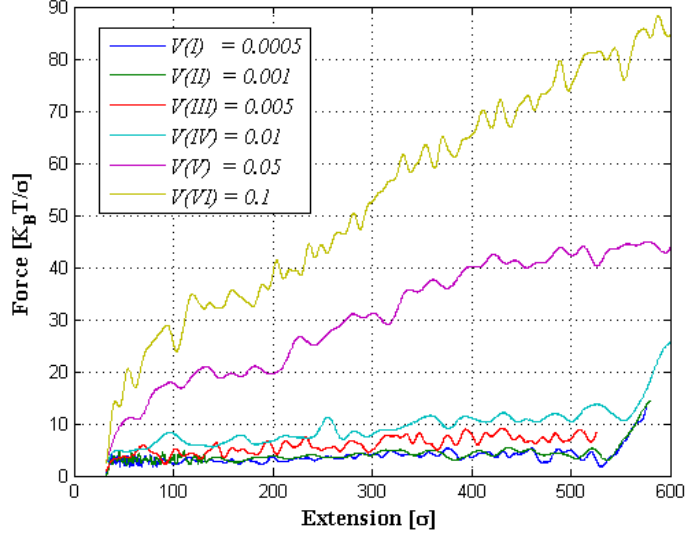


Figure 3-10: Filtered Force-extension curves plotted with different pulling velocities at $V(I) = 5 \times 10^{-4}$, $V(II) = 1 \times 10^{-3}$, $V(III) = 5 \times 10^{-3}$, $V(IV) = 1 \times 10^{-2}$, $V(V) = 5 \times 10^{-2}$, and $V(VI) = 1 \times 10^{-1}$. These FECs are calculated at the DNA end which is connected to the fake atom 2 which is moving a constant velocity.

velocity, the bigger the FEC's slope. This behavior has been found in a theoretical-simulation study [82]. In this study, a small uncharged semiflexible polymer was employed and it was found that the pulling velocity changes the FEC linearly. The authors argued that this linear behavior comes from the entropic elasticity. Figure 3-11 is the response of the DNA monomer which is connected to the fake atom which is fixed in the space. In the figure, only the responses at pulling velocities $0.005\sigma/\tau$, $0.001\sigma/\tau$, $0.01\sigma/\tau$, $0.1\sigma/\tau$ are plotted for the clarity of the picture. We observe that these curves oscillates around a constant value ($\approx 2.5k_B T/\sigma$) and the oscillation becomes stronger as the pulling velocity is higher. However, the linear

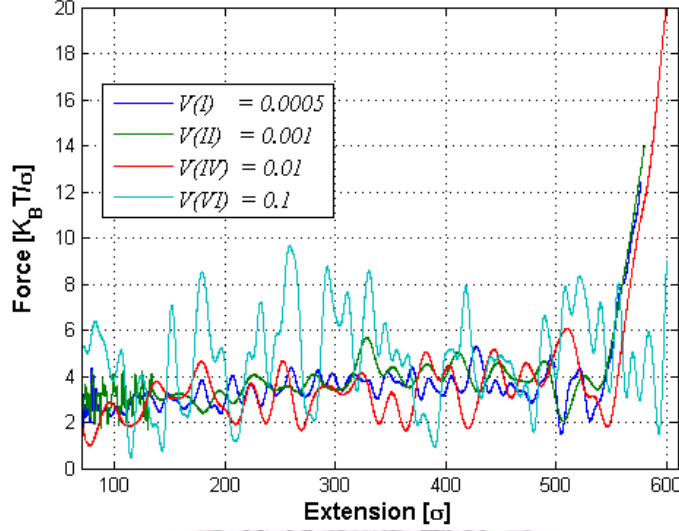


Figure 3-11: Filtered Force-extension curves plotted with different pulling velocities at $V(I) = 5 \times 10^{-4}$, $V(II) = 1 \times 10^{-3}$, $V(IV) = 1 \times 10^{-2}$, and $V(VI) = 1 \times 10^{-1}$. The other velocities are not plotted here for the clarity of the picture. These FECs are calculated at the DNA end which is connected to the fake atom 1 which is fixed in a position.

behavior found at the other end is not found at this end. We observe that the responses of the DNA molecule at velocities $0.005\sigma/\tau$ and $0.001\sigma/\tau$ are, at both ends, almost the same. This indicates that the DNA is being stretched in a “quasi-equilibrium” state and it is not perturbed by these velocities. It is important to mention when a polyelectrolyte is being stretched, it should have at least a time to relax in the order of the Rouse relaxation time. In Figure 3-12, we show that the influence of the pulling velocity on the bond length is linear. This means that the total contour length of the DNA grows linearly with the extension. The curves $V(I)$ and $V(II)$ basically have the same behavior. However, the curves $V(III)$,

$V(IV)$ starts growing faster with a higher slope than the others cases. The curves $V(V)$ and $V(VI)$ show that the dynamics of the complex is strongly influenced for the high pulling velocity which changes its internal structure. We find that the magnitude of the pulling velocity influences the force profile (the nature of the elastic response) and the internal structure of the complex (bond length). Furthermore, it is very important to choose an adequate pulling velocity, which does not perturb the system and allow the complex to relax and follow its natural behavior when it is stretched. As depicted in Figure 3-10 and 3-11, the $V(I) = 5 \times 10^{-4} \sigma / \tau$ does not perturb the complex at the two ends. Moreover, when the velocity is much smaller than the reference value, V_o , the responses of both DNA ends are basically identical; the complex is being stretched in an “quasi-equilibrium” state and this velocity does not change the natural behavior of the condensed DNA molecule. The value of $V(I) = 5 \times 10^{-4} \sigma / \tau$ is hence set as the pulling velocity in the following simulations.

3.5 Force-extension curve (FEC)

We analyze the FEC in this section. Figure 3-11 shows the FEC of the DNA which was stretched at different velocity including $V(I) = 5 \times 10^{-4}$. This figure clearly shows that the elastic response of the condensed DNA molecule differs from the WLC model. Experiments [5, 6, 7] have described that “plateau force” should appear for $C \sim C_c$ and “stick-release behavior” for $C_c < C \sim C_o$. We recall that C_c is the condensation threshold, C_d is the decondensation threshold and C_o is defined as the concentration in which the DNA molecule is totally neutralized. In experiments, C_o is much larger than the minimum number of particles required to neutralize a specific DNA molecule. This is because the presence of the monovalent salt in the solution whose concentration in biological conditions is in the same order

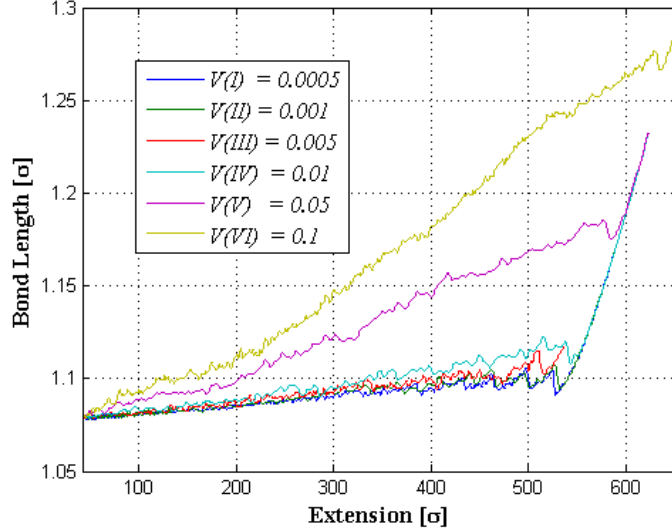


Figure 3-12: Bond length curves plotted with different pulling velocities at $V(I) = 5 \times 10^{-4}$, $V(II) = 1 \times 10^{-3}$, $V(III) = 5 \times 10^{-3}$, $V(IV) = 1 \times 10^{-2}$, $V(V) = 5 \times 10^{-2}$, and $V(VI) = 1 \times 10^{-1}$ as a function of the DNA extension.

of C_d ($C_d/C_c \sim 10^3$ to 10^4) [14]. Furthermore, C_c grows linearly with increasing the monovalent salt concentration, which shifts C_o to a higher value; however C_d is almost independent on the monovalent salt concentration [83]. For our case, the neutralizing point can be estimated as $N_{DNA}/Z_{SP} = 128$ which corresponds to a concentration of $C_o \approx 5 \times 10^{-5} \sigma^{-3}$. Indeed, we observe in our simulations that the DNA molecule is totally neutralized at this concentration.

3.5.1 N_L and N_R

When the DNA is being stretching, there is still a delicate issue to consider. At the beginning of this process all the DNA monomers form a toroid (See Figure 3-6);

the complex then starts forming a rod-toroid-rod structure as shown in Figure 3-8. Here, we divide the stretched DNA molecule into three parts, rod (part I), toroid (part II) and rod (part III). During a stretching process, the DNA form a rod-like structure from the first DNA monomer to N_L^{th} DNA monomer (this is the part I); then from the N_L^{th} DNA monomer to N_R^{th} DNA monomer, it forms a toroid-like structure (this is the part II); and finally from the N_R^{th} DNA monomer to the last DNA monomer, it forms a rod-like structure again (this is the part III). This brings up an interesting question of how we split these three parts and determine N_L and N_R (See Figure 3-17). We propose the following algorithm (refer to Figure 3-13 as an example). First, we project the DNA's bond vector in the stretching direction (x-axis). If this projection changes its sign, it means that the DNA made a half turn (semi-circumference) at this point. Thus, each time the DNA forms a loop, the x-component of the bond vector has to change its sign twice. This behavior persists until the DNA has formed the last loop as shown in Figure 3-13. In Figure 3-13 the projection of bond vector is plotted with its smoothing and discrete curve. The smoothing curve, SBL , was obtained by using an Adjacent Averaging algorithm which takes the average of a specific number of data points around each point in the data and replaces that point with the new average value. The discrete curve, DBL , was obtained by setting each positive value of SBL to 1 and each negative value of SBL to -1. This is done here to calculate how many times the DNA wraps around to a specific axis. Then, we estimate how many turns the toroidal part of the DNA has by counting the number of changes over 2 in the discrete curve, DBL ; this is also called "the winding number". However, we cannot calculate N_L and N_R yet because when the projection of the bond vector changes its sign for the first time or for the last time the DNA has already formed or not completely formed a half loop. In order to solve this problem, we make the following approximation. By knowing the position

of DNA monomers where the projection of the bond vector changes its sign for first and for last time, we calculate the maximum and the minimum of the x-component between all the DNA monomers in the toroid-like structure region. The minimum x-component corresponds to N_L^{th} DNA monomer going from the first monomer and the maximum x-component corresponds to N_R^{th} DNA monomer coming back from the last DNA monomer. The position of N_L and N_R are determined in this manner. The position of DNA monomers, N_L and N_R , are shown in Figure 3-14 during the whole stretching process. The figure shows that the toroidal DNA prefers to stay close to the first monomer (the center of mass of the toroidal part is close to it). The number of monomers inside the toroidal DNA decreases almost linearly (See Figure 3-15). In Figure 3-16, we show the winding number calculated by the two methods: the Eq. 3.9 and the approximation described lines above. We see that the two techniques give consistent results. Both of them show that the DNA loses one loop each time at the same position. The difference of the results obtained by the two methods comes from that our approximation of counting how many times the x-component of the bond vector changes only gives integer because when the last half loop is formed it will not produce a change of sign; however the Eq. 3.9 gives the exact number of turns.

3.5.2 Stick-release behavior

In Figure 3-9, we have seen that the calculated force at both DNA ends are very sensitive to the bond length vibration. After applying the filter, we observed that the figure shows a plateau with peaks occurring frequently; however we cannot guaranty that these peaks are a natural response of the condensed DNA molecule or some artificial effect coming from the filter. Therefore, we analyze our system in another way in order to find an equivalent method to calculate the force applied on the DNA molecule reducing effectively the noise generated by the bond length

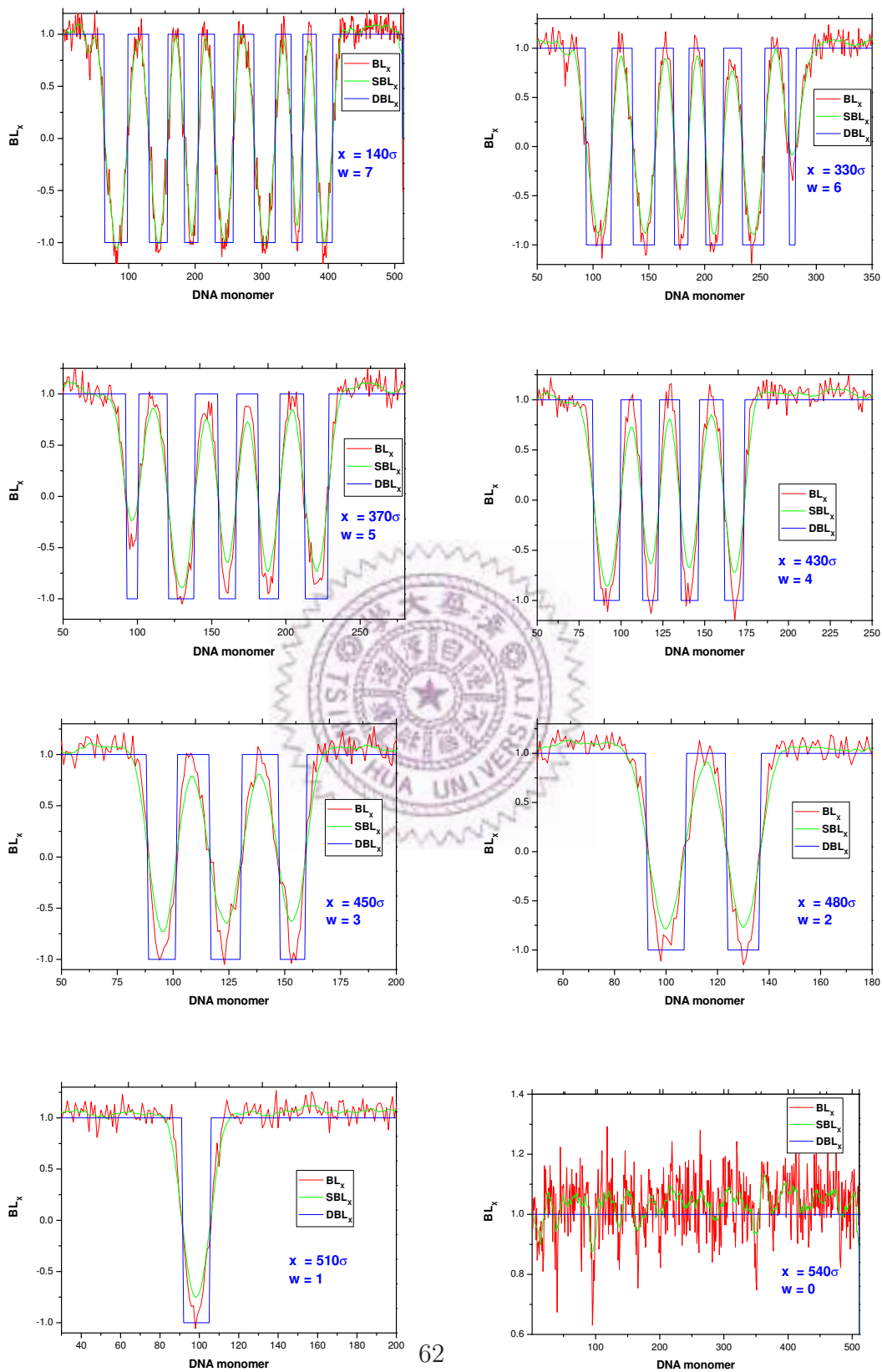


Figure 3-13: Projection of Bond vector in the direction of the pulling velocity as a function of the DNA monomer. The projection of Bond length is plotted with its smoothing curve, SBL , and discrete curve, DBL . Each curve has the extension and the winding number.

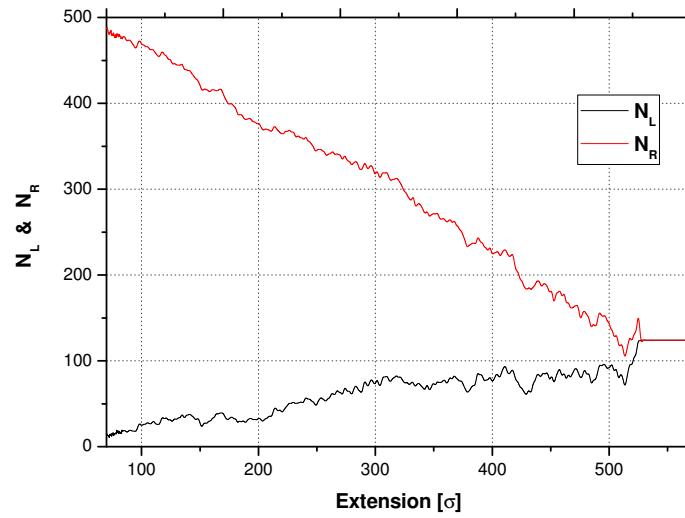


Figure 3-14: N_L and N_R as a function of the DNA's extension.

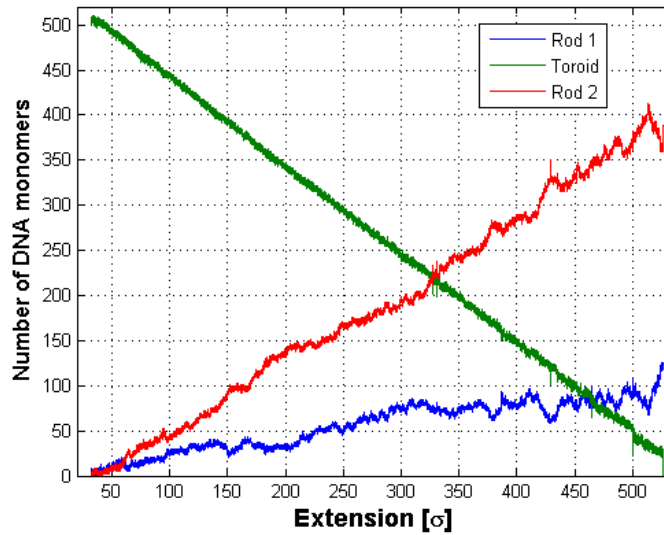


Figure 3-15: Number of monomers in each part of the DNA molecule as a function of DNA extension

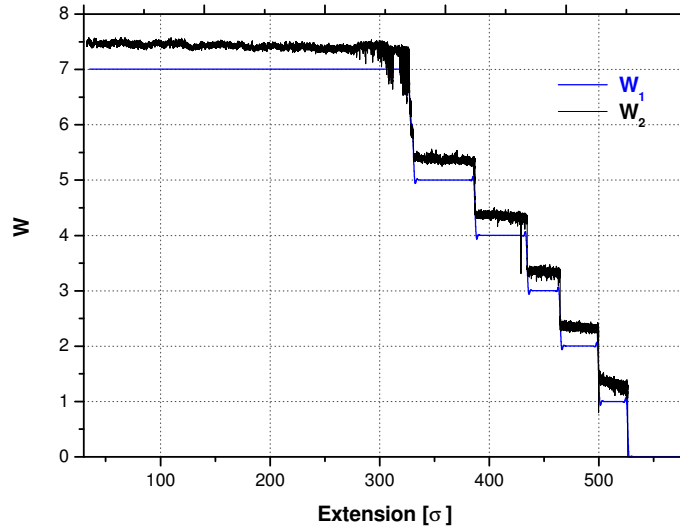


Figure 3-16: Winding number calculated by two methods. W_1 calculated by Eq. 3.9 and W_2 calculated by the algorithm proposed in the Subsection 3.5.1.

vibration at the same time. We consider the rod-like parts of our system as a line of beads which join each other by springs. The system moves only in the direction of the pulling velocity and is stretched in the equilibrium state at very low velocity, as shown in Figure 3-17. In these conditions, the acceleration of each DNA monomer would be very small or even zero. Thus, the force applied at one DNA end would be equal to the force applied on the springs connecting the DNA monomers and the total force on each monomer would be zero.

Figure 3-18 shows that the bond length in the part II of the DNA remains almost constant until the DNA is fully stretched. It suggests that when the DNA condenses into a toroid-like structure the equilibrium bond length shrinks in to a value of 1.0823σ and is nearly not perturbed in the whole stretching process. This value, $b = 1.0823\sigma$ (in the part II), is a little bit smaller than the bond length in our initial setup, $b_o = 1.1\sigma$ due to the condensation of tetravalent counterion

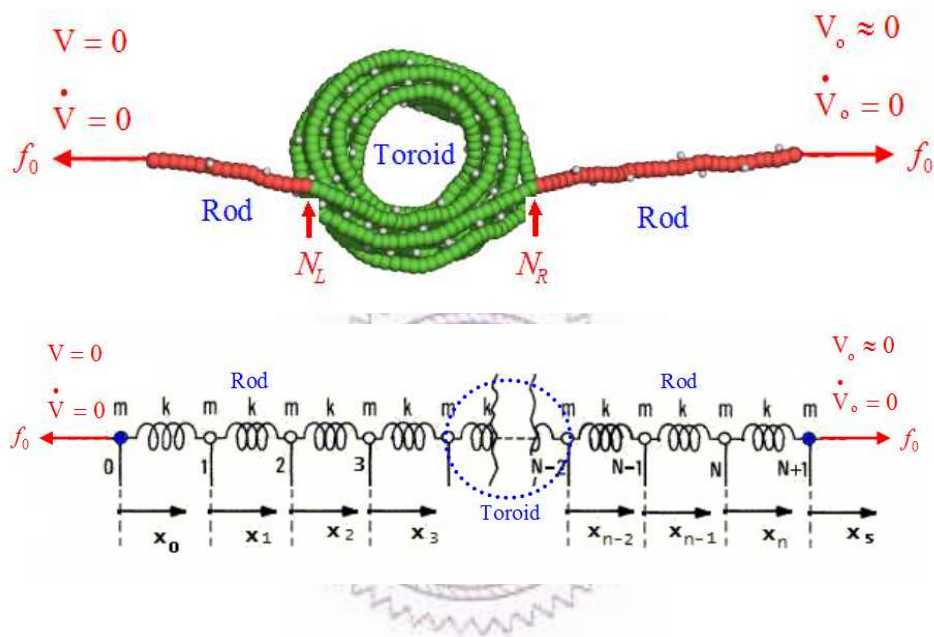


Figure 3-17: Condensed DNA molecule and its simplified model of the stretching process. The pulling velocity is $V_0 \approx 0$ so that the complex is stretched in an equilibrium state. The figure also shows the index of DNA monomers, N_L and N_R , where the DNA molecule forms a toroidal structure.

on the chain; however in the rod-like parts (part I and part III), the average bond lengths oscillate around 1.1σ . We observe that the bond length in the part I and part III has the same behavior, which implies that the force in part I and part II are the same. This supports our simplified model. Moreover, the bond length of the part I and part III shows a stick-release pattern when every time the DNA loses one turn. Keeping this on mind, we change Eq. 3.10 to

$$\langle F_x \rangle = -2k \frac{\langle d \rangle - b_o}{\langle d \rangle} \langle d_x \rangle \quad (3.13)$$

where b_o is set to the value of the equilibrium bond length in the condensed state, $b_o = 1.083$, $\langle d \rangle$ is the average distance between monomers and $\langle d_x \rangle$ is its projection in the stretching direction (x-axis). $\langle d \rangle$ and $\langle d_x \rangle$ are calculated by

$$\langle d \rangle = \sum_{i=1}^{N-1} \frac{\sqrt{(x_{i+1} - x_i)^2 + (y_{i+1} - y_i)^2 + (z_{i+1} - z_i)^2}}{N-1} ; \quad (3.14)$$

and

$$\langle d_x \rangle = \sum_{i=1}^{N-1} \frac{(x_{i+1} - x_i)}{N-1} \quad (3.15)$$

We recalculate the force by using Eq. 3.13 and plot it together with the force obtained by the Eq. 3.10 (at $v_o = 5 \times 10^{-4}$ connected to the fake atom which was fixed in the space) and the results are shown in Figure 3-19. In the figure, we clearly see that both curves match well in the whole range of the DNA extension. The four last peaks in each curve happens at the same position and they roughly have the same amplitude. These mean that the DNA molecule experiences a tension drops when every time it loses a turn. Moreover, these peaks represent the natural response of the DNA molecule. This is the “stick-release pattern” observed in experiments. Both of the two curves show a plateau force until $x \approx 300\sigma$, right after that the force gradually increased with increasing extension, then abruptly

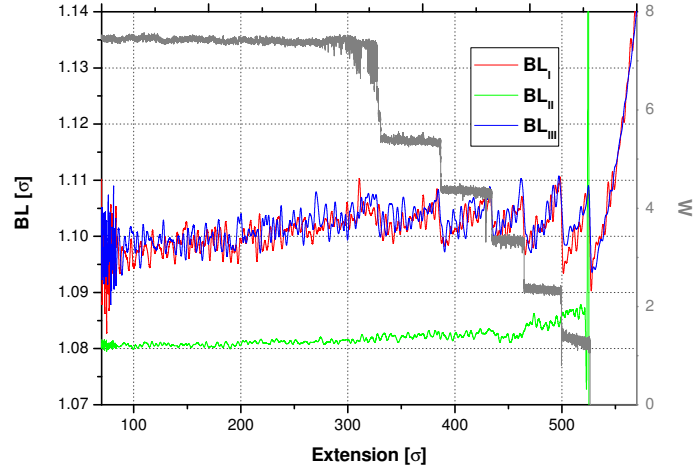


Figure 3-18: Bond length, BL , and Winding number, W , as a function of the DNA's extension. This figure clearly shows that the bond length has similar behavior as force-extension profile.

decreased during stretching, and this behavior appears repeatedly and becomes stronger and stronger after the DNA loses its third loop. In the range of $x = 0$ to $x = 526\sigma$ the entropic behavior of the DNA molecule is strongly affected by the condensed counterions. Moreover, each peak has a duration of one turn which can be seen either from bond length curve in Figure 3-18 or from force curve in Figure 3-19. This suggests that these "stick-release patterns" are a consequence of turn-by-turn unfolding of the condensed DNA toroid. Right after $x \approx 526\sigma$, the elastic response of the DNA molecule can be described by the Extensible Worm-Like Chain (EWLC) model [64].

$$\frac{FP}{k_B T} = \frac{\langle x \rangle}{L} + \frac{1}{4(1 - \langle x \rangle/L + F/K_o)^2} - \frac{1}{4} - \frac{F}{K_o} \quad (3.16)$$

We observe that DNA molecule starts following the EWLC model when it completely loses all its turns and it is in the extended-coli state. The FEC is

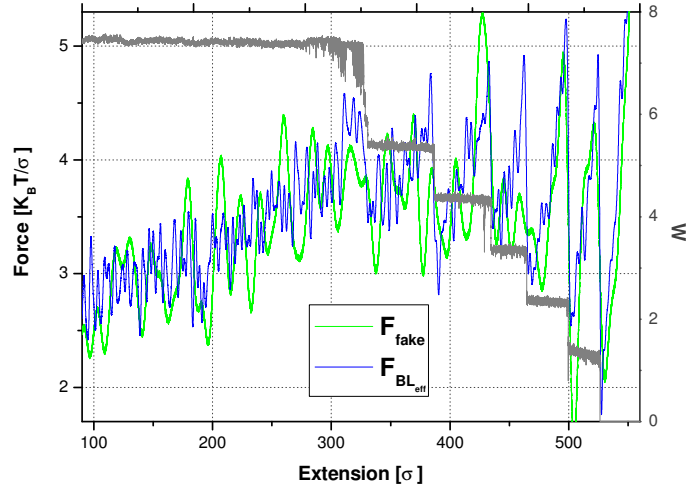


Figure 3-19: Response of single condensed dsDNA molecule to an applied force. The FECs were calculated by using the two techniques. The EWLC model can only describe the stretching process when the extension of the DNA is close to the overall contour length.

fitted to the EWLC equation 3.16 in the range of $x = 526\sigma$ to $x = 587\sigma$ by using a Levenberg-Marquardt algorithm (LMA). This algorithm gives $L = 559.7\sigma$, $P = 25.2\sigma$ and $K = 230.2k_B T/\sigma$ as results. The contour length, L , obtained by fitting the curve is very close to the initial contour length of our DNA molecule, $L_o = (N_{DNA} - 1)b_o = 562.1\sigma$ and the elastic modulus is $K_o = 2kb_o = 220K_B T/\sigma$ which is also close to fitting value, K . For a polyelectrolyte chain, the persistence length, P , is the sum of two components, one is the bare persistence length, P_o , coming from the intrinsic chain stiffness, and the other one is the electrostatic persistence length, P_e , due to electrostatic interaction. The intrinsic persistence length can be defined as the length of the chain segments which forms an arc of $1rad$ with a bond bending energy equals to $k_B T/2$. For a quartic bond-angle potential, the intrinsic persistence length can be obtained by solving the following

equation

$$\left(\frac{P_o}{b_o}\right)^4 - 2\frac{k_1}{k_B T} \left(\frac{P_o}{b_o}\right)^3 + 2\frac{k_1}{k_B T} \left(\frac{P_o}{b_o}\right)^2 - 2\frac{k_2}{k_B T} \left(\frac{P_o}{b_o}\right) + 2\frac{k_2}{k_B T} = 0 \quad (3.17)$$

The intrinsic persistence length is $P_o = 11.78\sigma$. In our simulation, the persistence length of the condensed DNA is $P_c = 11.25\sigma$, estimated from the average radius of the DNA toroid. These two values, P_o and P_c are consistent because the DNA is neutralized by the condensed tetravalent counterions and as a consequence only the intrinsic chain stiffness plays an important role in determining the size of the condensed DNA. Moreover, we recall that the simulation in the Section 3.3.1 in which a short DNA chain, $N_{DNA} = 256$, was condensed at its neutralizing point, $N_{SP} = 64$, and the results also show that the average radius of the condensed DNA is $R \approx 11\sigma$. These imply that the persistence length of the condensed DNA should be the same to the intrinsic persistence length at the neutralizing point, independent of chain length ($P_o \approx P_c$). Furthermore, we can estimate the electrostatic persistence length from the value of $P = 25.21\sigma$ which is the persistence length of the DNA molecule in the coil-extended state. The electrostatic persistence length is $P_e = P - P_c \approx 13.43\sigma$. Figure 3-20 shows the FEC and its fitting curve. We see that these curves match well in the fitting range of $x = 526\sigma$ to $x = 587\sigma$ with the goodness-of-fit parameter equals to $R^2 = 0.98413$.

However, it is still unclear about why the DNA loses its first turn late, for example in our case it is close to $x \approx 300\sigma$, and why it does not happen earlier; moreover, why is the extension of each turn roughly the same ($\approx 35\sigma$) after the first turn is lost, as suggested by Murayama et al. [7]?. Murayama et al. stated that the collapse DNA has a structure with characteristic length of $0.3\mu m$ because the peak-peak distance measured from the stick release pattern was roughly $0.3 \pm 0.05\mu m$. In the following Sections, these questions will be discussed.

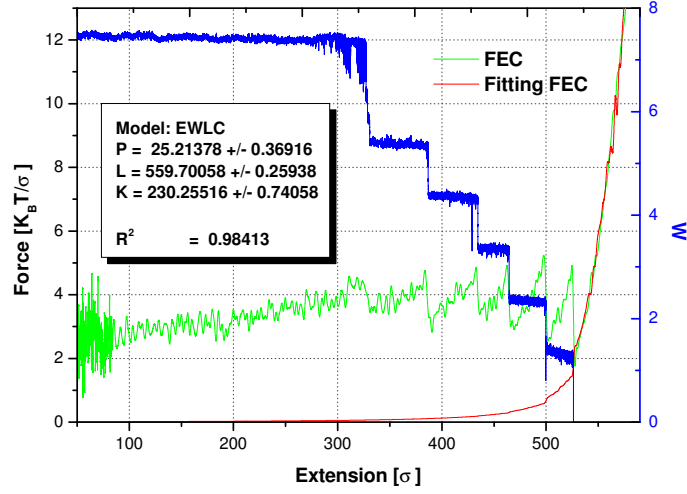


Figure 3-20: FEC fitted with the EWLC in the range of $x = 526\sigma$ to $x = 587\sigma$. R^2 is very close to one which corresponds to a perfect fit.

3.5.3 Asphericity

In the preview section, the study of the winding number suggests that the DNA unfolds turn by turn. Here, we discuss how the asphericity of the DNA molecule, As , in the stretching process changes with the winding number. We recall that our DNA molecule was divided into 3 parts: part I (rod), part II (toroid) and part III (rod). We monitor the As in this three parts. We know that the asphericities are 1 and 0.25 for a perfect rod and a ring, respectively. Figure 3-21 shows the As for the three cases. The asphericity for the part I and part III are close to one, $As_I \approx As_{III} \approx 1$, as it was expected because during the simulation they have a rod-like structure. The asphericity for the part II shows a periodicity which is related to the winding number (plotted in the same figure). In the previous sections we have seen that each time the DNA loses one turn, the force decreases its value; however the asphericity shows opposite trend, it abruptly increases when one turn is lost. The asphericity for the part II is calculated here by two different ways.

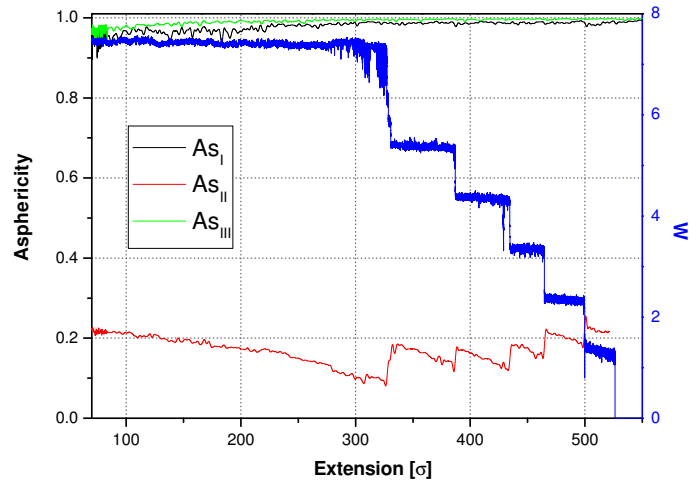


Figure 3-21: Asphericities plotted for the three parts: part I (rod), part II (toroid) and part III (rod).

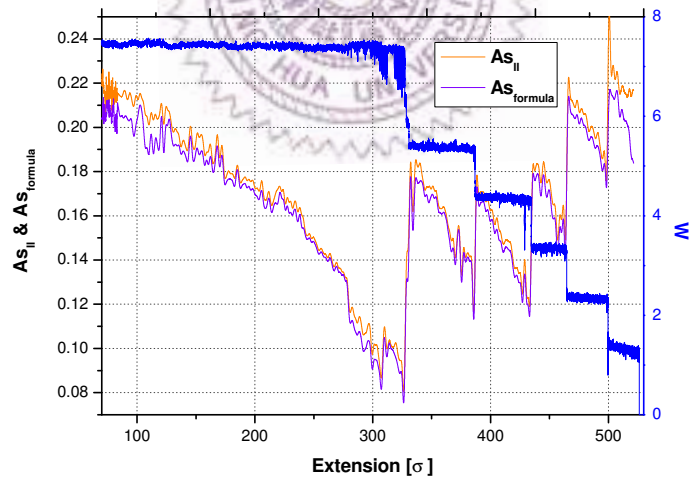


Figure 3-22: Asphericity in the toroid-like structure (part II), calculated by two methods. As_{II} calculated by Eq. 3.5 and $As_{formula}$ calculated by Eq. 3.6

As_{II} is determined by using Eq. 3.5 and $As_{formula}$ is calculated by Eq. 3.6 which comes from the assumption that the DNA forms a perfect toroid (R is replaced by $(R_1 + R_2)/2$ in Eq. 3.6). The results are plotted together in Figure 3-22. This is done to understand the behavior of DNA molecule in the region of part II. We see that these two curves are almost the same which means that our approximation for Eq. 3.5 works well. For a DNA forming a toroid, it is reasonable to think that r_o will not be larger than R . The largest r_o can be roughly $R/2$. It means that r_o/R is in the range of $[0, 1/2]$. In Eq. 3.6, if the ratio of r_o/R is zero, As_{II} becomes 0.25 (ring) and if the ratio, r_o/R , is $1/2$, As_{II} becomes 0.09. These are the bounds for being a toroid. However, when the first loop is lost the asphericity is a little bit smaller than our lower bound. We observe from the movie that the DNA has a solenoid-like structure, where r_o is the height and is almost equal to R in this region ($x = 305\sigma$ to $x = 325\sigma$). After that, the DNA attains a toroidal shape in the part II as shown in Figure 3-22. We observe that As_{II} starts decreasing from its equilibrium value $\langle As \rangle \approx 0.2177$, then increases abruptly when one loop is lost. This behavior is repetitive during the stretching process. As_{II} finally reaches a value very close to 0.25 before the toroidal part disappears. This is because the DNA is losing one turn by one turn that becomes similar to ring for the last turn.

3.5.4 Minor radius, r_o , and major radius, R

In this section, we study the internal structure of the DNA in the part II (toroid). We measure the size of the minor radius, r_o , and the major radius, R (R_1 and R_2). In Figure 3-23, we clearly see that the condensed DNA molecule first decreases its size linearly with a constant rate; however the minor radius is kept fixed until the major radius meets the minor radius ($R \approx r_o$), which is the minimum size. At this point, the complex is not stable (as also shown in Figure 3-22) and as a consequence the complex needs to lose one turn to become stable. The size of R

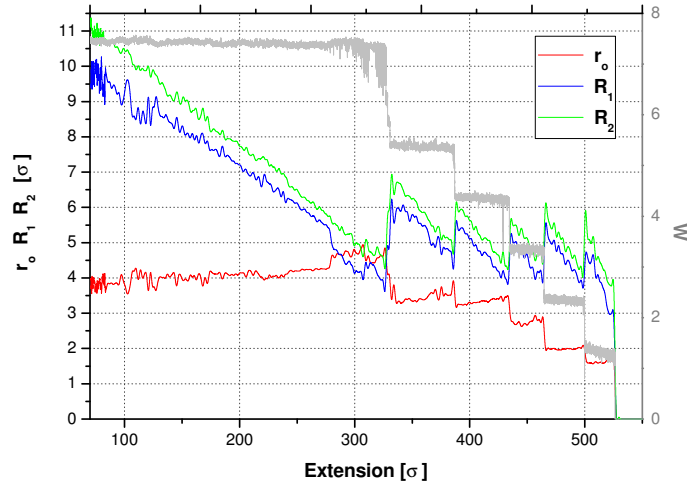


Figure 3-23: Internal parameters of a DNA during the stretching process. The minor radius (r_o) and the major radius (R_1 and R_2) plotted together with the winding number (W)

then increases rapidly and it starts decreasing linearly with the same speed to the its minimum size again; however r_o decreases in a stepwise fashion. This behavior is permanently until there is no loop in the part II. This minimum size might depend on the monovalent or multivalent salt concentration. The complex, in this part, always displays a toroid-like structure. It is important to mention that our methodology of computing the eigenvalues and then estimating the value of R , calculates the average radius of all the toroid. The average radius also includes the size of the turn which is being reduced. It suggests that the DNA loses its first turn late because the DNA first needs to reduce its size to an a minimum value ($R_{min} \approx 6\sigma$) at the beginning, then keeps this size and starts decreasing only the size of one turn until the turn disappears. In this case, the extension of the periphery of each turn should be roughly the same, $Length = 2\pi R_{min} \approx 37\sigma$, because each turn starts reducing its size from the minimum radius. This confirms

the Murayama's suggestion [7] and shows that the condensed DNA after reducing its size has a characteristic size. It is logic to think that r_o only decreases when one turn is lost because the thickness of the toroidal part depends on the number of turn. All of these demonstrate that the DNA unfolds turn by turn for the “stick-release patterns”.

3.5.5 Effective fractional extension, x/L_{eff}

Wada et al. [8] proposed a model for the plateaus force. They formulated that as long as the fractional extension (x/L) would not change in equation A.5, the force (F) would remain constant. Here we see what happen to the “stick-release pattern”. In Figure 3-24, we observe that the dependence of the effective contour length over extension is almost linear, which would suggests that our FEC should be a constant force because $x/L_{eff} \approx const$. However, care should be taken in this study. While using equation A.5, we realize that a small change in x/L_{eff} would produce a big change on the force. In order to know this, we plot the effective fractional extension, x/L_{eff} , over extension in Figure 3-25. We observe that every time the DNA loses a turn there is a sharp decrease in the ratio x/L_{eff} and this effect becomes strong specially in the last three turns. We know that x decreases linearly so L_{eff} has to increase abruptly to reduce this ratio, x/L_{eff} , which corresponds to the moment that one turn is lost. This suggests that the general WLC model can be used to understand this phenomenon because as we mentioned before a small change in x/L_{eff} would produce a big change on the force, specially when this ratio is very close to 1.

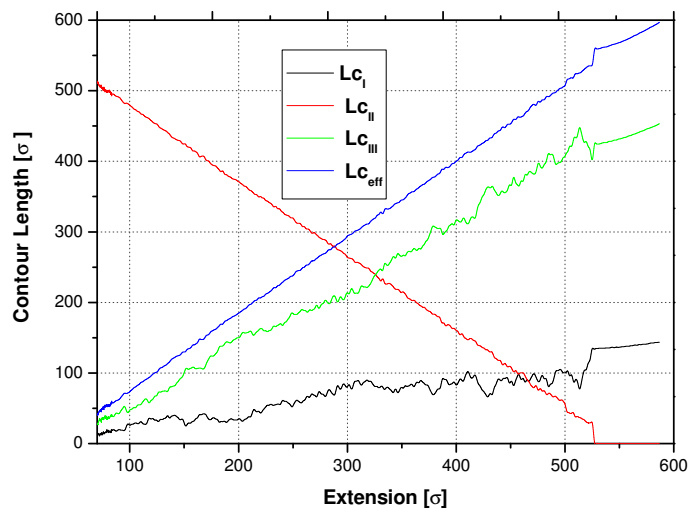


Figure 3-24: Effective contour length plotted for the three parts: part I (rod), part II (toroid) and part III (rod).

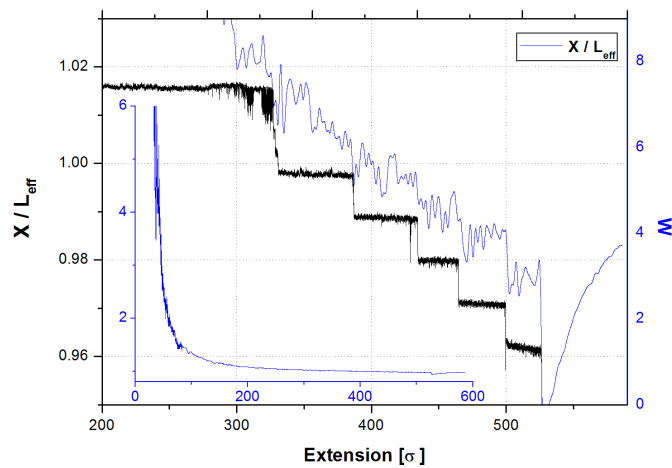


Figure 3-25: The effective fractional extension plotted together with the winding number. The inset shows the variation of the effective fractional extension in all the extension range.

3.6 How do our results depend on different initial configuration?

Our previous simulations were done using only a specific initial configuration. Here we choose five different configurations of the condensed DNA toroid in the equilibrium state in order to verify the dependence of the initial configuration over the DNA behavior in the stretching process. The results are plotted in Figure 3-26. We see that the initial configuration does not influence the whole stretching process. Moreover, the DNA molecule loses each turn roughly at the same position which implies that DNA basically reduce its size to a minimum value then starts losing one by one loop. These results indicates that the position where each turn is lost might depend on the monovalent or multivalent salt concentration as mention in the subsection 3.5.4.

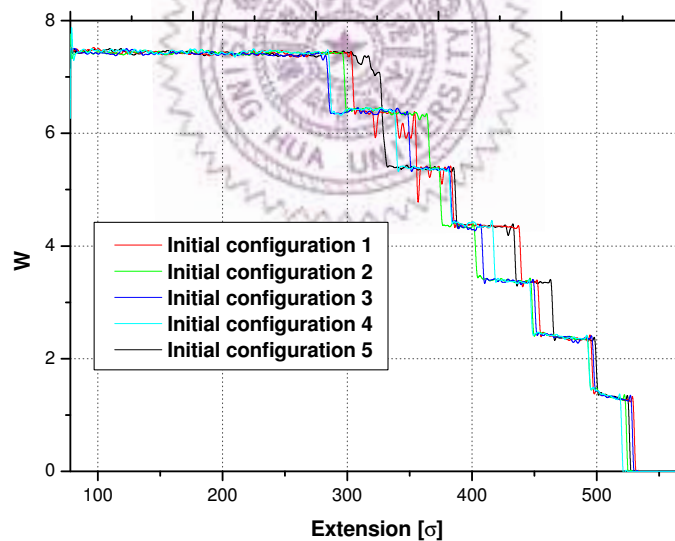
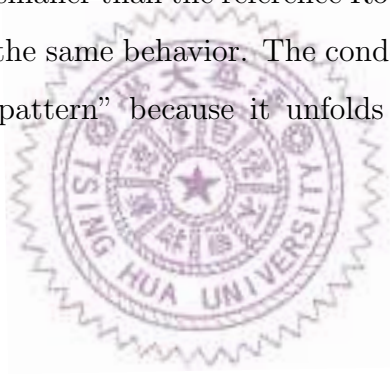


Figure 3-26: Winding numbers plotted together with different initial configurations.

3.7 Snapshots of our condensed DNA toroid during the stretching process

In this Section, we show the snapshots of our condensed DNA molecule being stretched. We recall that our simulation mimics the experiments [5, 6, 7] in which a condensed DNA molecule was stretched by using optical tweezer. We measure the FEC in the stretching process by trapping one faked atom and pulling the other faked atom at constant velocity (These two faked atoms are tethered to the free DNA ends). The extension was determined from the distance between the two faked atoms centers and the force acting on our DNA molecule was determined from the displacement of the DNA end from the fixed faked atom. However, we showed that for a velocity smaller than the reference Rouse velocity, V_o , the profiles at both ends should have the same behavior. The condensed DNA toroid presents a series of “stick-release pattern” because it unfolds turn-by-turn as shown in Figure 3-27.



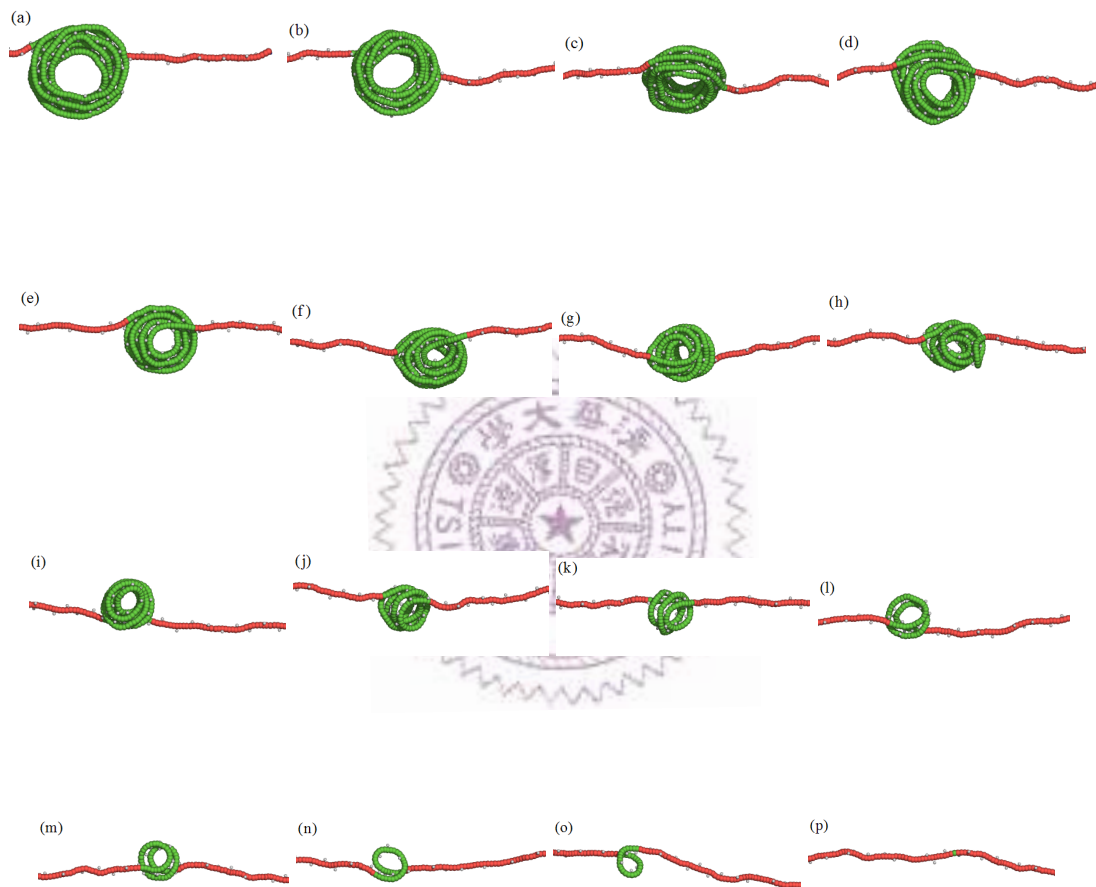


Figure 3-27: Snapshots of a single condensed DNA toroid during a stretching process.

Chapter 4

Conclusion

DNA condensation and its stretching process was studied by means of molecular dynamics simulation. A coarse-grained model was employed to model the double helix DNA molecule and the spermine (tetravalent counterions). The relation between the counterion size and DNA monomer size was studied by varying systematically their diameter. We found that for $r_{DNA} = \sigma$ and $r_{SP} = 0.5\sigma$, the complex formed a well-defined toroidal structure. Then, the morphology of a condensed DNA was investigated. We found that the initial configuration of the DNA does not influence the final conformation. The two major radii, (R_1, R_2) , and minor radius, r_o , of the condensed DNA toroid were measured. We found that R_1 and R_2 are basically the same, independent of the chain length or counterion concentration, which means that the toroid grows to a characteristic size at the neutralizing point (C_o). Moreover, if the initial spiral radius is far from the characteristic radius of the toroid, the simulation takes more time to reach the equilibrium state. The decondensation transition of a condensed DNA molecule was investigated by stretching the condensed DNA out. MD simulation was performed at different stretching velocities to study the effects of the pulling velocity on the FEC. We found that the pulling velocity influences the force profile (the

nature of the elastic response) and the internal structure of the complex (bond length). If the pulling velocity is high, the condensed DNA chain experiences a rapidly transition between being condensed and becoming extended where its dynamics are drastically changed by a high pulling velocity. Moreover, we found that the responses at both DNA ends are different if the pulling velocity is larger than the reference Rouse velocity, $V_o = 1.68 \times 10^{-3} \sigma / \tau$. For the velocities larger than V_o , the FEC's dependence over the pulling velocity is linear at the DNA end which is moving at constant velocity. It means that the higher the pulling velocity, the bigger the FEC's slope. At the another DNA end (fixed in the space), the linear behavior is not found; nevertheless these FECs oscillate around a constant force ($\approx 2.5K_B T / \sigma$) and the oscillation becomes stronger and stronger as the pulling velocity is much larger than V_o . For velocities much smaller than V_o , the responses at both ends are basically the same. We found that a pulling velocity equals to $5 \times 10^{-4} \sigma / \tau$ does not perturb the complex, which indicates that the DNA is being stretched in a "quasi-equilibrium" state. It is worth to notice that when a polyelectrolyte is being stretched, it should have at least a time to relax in the order of the Rouse relaxation time. We found that the influence of the pulling velocity on the bond length is linear for all the velocities. The bond length's slope increases as long as the pulling velocity is risen to a high value. We found that the entropic behavior of the DNA molecule is strongly affected by the condensed counterions in the range of $x = 0$ to $x = 526\sigma$. We observed that our FEC presents a plateau force until $x \approx 300\sigma$; the force gradually increased with increasing extension, and then abruptly decreased during stretching and this behavior appears repeatedly and becomes stronger and stronger as soon as the DNA molecule is losing its turns. This behavior was observed in experiments and was called "stick-release patterns"; however there was no a direct evidence about why the DNA shows this kind of FEC. We showed that these "stick-release patterns" are a consequence

of turn-by-turn unfolding of the condensed DNA toroid. When the DNA's last loop disappears, the FEC starts following the EWLC model. This FEC was fitted to the EWLC equation in the range of $x = 526\sigma$ to $x = 587\sigma$ by using a Levenberg-Marquardt algorithm (LMA). The results are $L = 559.7\sigma$, $P = 25.2\sigma$ and $K = 230.2k_B T/\sigma$. We found that the values of L and K , obtained by fitting, quite agree with the theoretical values, the initial contour length, $L_o = 562.1\sigma$ and the elastic modulus, $K_o = 220k_B T/\sigma$. We found that the intrinsic persistence length, P_o , and the persistence length of the condensed DNA, P_c , are almost the same at the neutralizing point because counterions are condensed that they reduce effectively the charge on the DNA which starts behaving as a neutral chain and only the intrinsic chain stiffness plays an important role in determining the size of the DNA molecule. We divided our DNA molecule into 3 parts: part I (rod), part II (toroid) and part III (rod). We found that the asphericities in each part I (As_I) and III (As_{III}) are very close to 1 which means that these parts always have a rod-like structure. We found that the asphericity in part II starts decreasing from its equilibrium value $\langle As \rangle \approx 0.2177$, then increases abruptly and this behavior is repetitive each turn is lost. As_{II} then finally reaches a value very close to 0.25 before the toroidal part disappears which means that the DNA is losing one turn by one turn and becomes a perfect ring. The internal structure of the condensed DNA molecule ($R, r_o, x/L_{eff}$) was investigated during the whole stretching process. We found that the condensed DNA molecule first decreases its major radius, R , linearly with a constant speed to a minimum size (This minimum size might depend on the monovalent or multivalent salt concentration). Then, the condensed DNA molecule (part II) keeps this minimum size and starts decreasing only the size of one turn until it disappears. It then continues with the other turns in the same manner; however the size of minor radius is kept constant until the major radius meets it, and then it starts decreasing in a stepwise fashion. We found that

every time the DNA loses a turn there is a sharp decrease in the ratio x/L_{eff} . Finally, we verified that our results are independent on the initial configuration. Five independent simulation with different initial configuration were stretched and the results show that the DNA molecules lose their turns almost at the same position.

We also explain the mechanism of the “stick-release patterns” formation in the FEC. Moreover, our results provide new information about the internal structure of a single condensed DNA toroid being stretched. Our results are in qualitative agreement with experiments. To understand the elastic properties of dsDNA is an important challenge for both experimentalists and theorists. Present research offers a route to understand DNA physics via the pathway of molecular dynamics simulation.



APPENDIX



Appendix A

The Worm-Like Chain

A variety of biological macromolecules such as DNA, RNA, and polypeptides are aimed to be described by the worm-like chain (WLC) model, proposed by Kratky and Porod [84]. Moreover, Bustamante et al. [63] have shown in their widely cited work that the WLC model can reproduce the force-extension curve (FEC) of a single λ -DNA molecule. The WLC model is a continuously elastic rod, used to represent the “isotropic behavior” of semiflexible polymers. The advantage of this model is that the chain length and the chain stiffness can be varied independently which allows more freedom in the treatment of Gaussian and non-Gaussian chain statistics. At the same time, it also avoids the use of the concept of statistical segments, where the division of a polymer into segments can be arbitrary and most of the time unrealistic. However, the WLC model does not consider the enthalpic elasticity contribution that is observed in most experiments.

A.1 Theory

To start modeling a polymer, it is needed to know the scale in which the polymer can be consider as rigid rod. It is natural to think that the DNA is a continuous

line with finite resistance to bending. This is the essence of the WLC model whose formulation treats the polymer as a continuum elastic rod with a fixed contour length (inextensible chain). To form the polymer, $N + 1$ identical backbone atoms are connected by N bond vectors, b_i where $i = 1, 2, \dots, N$, under the assumption that $b \rightarrow 0$ and $L \rightarrow \infty$. Furthermore, the chain is subjected to an equilibrium force, F , acting on the end-to-end distance vector, and its configuration is represented by the vector position, $\vec{r}(s)$, which is a function of the contour length S . The local tangent vector, $\vec{t}(s)$, and curvature vectors, $\vec{w}(s)$, are given by

$$\vec{t}(s) = \frac{d\vec{r}(s)}{ds}, \quad \vec{w}(s) = \frac{d\vec{t}(s)}{ds} \quad (\text{A.1})$$

the inextensibility condition of the chain is imposed with the constraint, $|\vec{t}(s)| = 1$. The energy, E , in the WLC model, for a stretched DNA molecule is a line integral along the DNA, and it comes from the contribution of two important terms A.2. The first term is the resistance of the chain to be bended. The second term is given by the opposition to be stretched and it is a result of applied force. Combining these contribution, the energy can be expressed as

$$E_{WLC} = \int_0^L ds \left(\frac{k_B T P}{2} \left| \frac{d\vec{t}(s)}{ds} \right|^2 - F \cos(\theta(s)) \right) \quad (\text{A.2})$$

where $\theta(s)$ is the angle between $\vec{t}(s)$ and the end-to-end distance vector of the polymer, and P is the persistence length of the chain, which is the characteristic length scale associated with the decay of tangent-tangent correlations at zero stretching force by

$$\langle \vec{t}(0) \vec{t}(s) \rangle \sim \exp\left(-\frac{|s|}{P}\right) \quad (\text{A.3})$$

the partition function is given by the path integral

$$Z(L, F, \vec{t}(0), \vec{t}(L)) = \int D(t) \exp\left(\frac{-E_{WLC}}{k_B T}\right) \quad (\text{A.4})$$

where $D(t)$ is the integration measure functional space of the paths drawn on the unit sphere starting at the point $\vec{t}(s=0)$ and ending $\vec{t}(s=L)$. The FEC relation for the WLC model was obtained from equations A.2 and A.4 by using numerical techniques [63, 85], because, an analytic solution for WLC model is not currently known. The interpolation formula is most commonly written today as

$$\frac{FP}{k_B T} = \frac{\langle x \rangle}{L} + \frac{1}{4 \left(1 - \frac{\langle x \rangle}{L}\right)^2} - \frac{1}{4} \quad (\text{A.5})$$

The equation A.5 is an interpolation formula to the numerical solution. This formula is a nonlinear equation. At low extension, the force grows linearly in x with a slope $\frac{3k_B T}{2PL}$ and at high extension, the force diverges as $\frac{k_B T}{4P} \left(1 - \frac{\langle x \rangle}{L}\right)^{-2}$. For given extension, This interpolation formula approaches the exact solution at lower and intermediate forces; however it fails to describe forces between these two regimes. At low force, it displays the Hooke's law behavior as

$$\frac{\langle x \rangle}{L} = \frac{2FP}{3k_B T} \quad (\text{A.6})$$

A.2 Experimental results and their models

According to the experimental results, The fit of equation A.5 at intermediate forces is good up to $5pN$, above which the model keeps increasing quicker than the experimental data. Further modifications to the WLC model have introduced an enthalpic correction for higher forces [see table A.1]. This addition makes the model valid up to approximately 60 pN, at which point DNA undergoes a

Table A.1: DNA elasticity models

WLC Model	Interpolation Formula
Marko-Siggia [85]	$\frac{FP}{k_B T} = \frac{\langle x \rangle}{L} + \frac{1}{4(1-\langle x \rangle/L)^2} - \frac{1}{4}$
Odijk [86]	$\frac{FP}{k_B T} = \frac{1}{4(1-\langle x \rangle/L + F/K_o)^2}$
Modified Marko-Siggia [64]	$\frac{FP}{k_B T} = \frac{\langle x \rangle}{L} + \frac{1}{4(1-\langle x \rangle/L + F/K_o)^2} - \frac{1}{4} - \frac{F}{K_o}$
Bouchiat et al. [87]	$\frac{FP}{k_B T} = \frac{\langle x \rangle}{L} + \frac{1}{4(1-\langle x \rangle/L + F/K_o)^2} - \frac{1}{4} - \frac{F}{K_o} + \sum_{i=2}^7 \alpha_i \left(\frac{\langle x \rangle}{L} - \frac{F}{K_o} \right)^i$

structural phase transition and the force-extension relation changes quite rapidly back to a more Hookean form, extending up to 1.6 times its normal contour length before displaying further non-linearities. No one is sure what the structure of DNA is after undergoing this structural phase transition, or how exactly it is able to stretch so significantly, though it has been proposed that the bases flip out away from the phosphate backbone, there is still a lot of work to do on the elastic properties of DNA.

The elasticity of DNA can be parameterized by 3 quantities, its initial contour length, L , its persistence length, P , and its elastic modulus, K_o . The persistence length measures the tendency to point in the same direction for a polymer. Moreover, the entropic behavior is dominant when the length of the polymer is much greater than its persistence length. The elastic modulus measures the intrinsic resistance of the polymer to longitudinal strain and it reflects enthalpic contributions. The table A.1 summarizes theoretical models for a polymer treated as WLC in which analytical expressions have been derived.

Marko-Siggia model is a purely entropic formula, and is valid for the lower range of forces, ($F < 5pN$), and differs from exact solution by up to $\sim 10\%$ near $F \approx 0.1pN$. Odijk model represents a combined entropic-enthalpic theory, applicable at large relative extensions, $|x - L_o|/L_o \ll 1$ for a force between the range,

$2pN < F < 15pN$. Modified Marko-Siggia WLC, also called Extensible Worm-Like Chain (EWLC), is entropic-enthalpic model of a polymer and incorporates enthalpic stretching. However it is limitedly similar to Marko-Siggia model near $F \approx 0.1pN$, and gives a good approximation up to $F < 20pN$. Bouchiat et al. WLC, which was obtained by using the rules of quantum mechanics and numerical methods, is claimed to have an accuracy better than 0.01% over the useful extension range, $0.06 \leq \langle z \rangle / L_o \leq 0.97$.



Bibliography

- [1] F. Miescher. Ueber die chemische Zusammensetzung der Eiterzellen. *Hoppe-Seyler's medicinisch-chemische Untersuchungen*, **4**:441, 1871.
- [2] J. Watson, and F. Crick. A structure for Deoxyribose Nucleic Acid. *Nature*, **171**:737, 1953.
- [3] V. Vijayanathan, T. Thomas, and T. J. Thomas. DNA Nanoparticles and Development of DNA Delivery Vehicles for Gene Therapy. *Biochemistry*, **41**:14085, 2002.
- [4] T. Nakamura, R. Moriguchi, K. Kogure, A. Minoura, T. Masuda, H. Akita, K. Kato, H. Hamada, M. Ueno, S. Futaki, and H. Harashima. DNA Nanoparticles and Development of DNA Delivery Vehicles for Gene Therapy. *Biol Pharm Bull.*, **29**:1290, 2006.
- [5] CG. Baumann, V. Bloomfield , SB Smith , C Bustamante , MD Wang , SM Block. Stretching of single collapsed DNA molecules. *Biophys J.*, **78**:1965, 2000.
- [6] Y. Murayama, and M Sano. Force Measurements of a Single DNA Molecule in the Collapsing Phase Transition. *J. Phys. Soc. Jpn.*, **70**:345, 2000.

- [7] Y. Murayama, Y. Sakamaki, and M Sano. Elastic Response of Single DNA Molecules Exhibits a Reentrant Collapsing Transition. *Phys. Rev. Lett.*, **90**:018102, 2003.
- [8] H. Wada, Y. Murayama, and M Sano. Model of Elastic Responses of Single DNA molecules in the Collapsing Transition. *Phys. Rev. Lett.*, **66**:061912, 2002.
- [9] M. Ueda and K. Yoshikawa. Phase Transition and Phase Segregation in a Single Double-Stranded DNA Molecule. *Phys. Rev. Lett.*, **77**:2133, 1996.
- [10] Y. Burak, G. Ariel, and D. Andelman. Onset of DNA Aggregation in Presence of Monovalent and Multivalent Counterions. *Biophys. J.*, **85**:2100, 2003.
- [11] H. Wada, Y. Murayama, and M Sano. Model of Elastic Responses of Single DNA molecules in the Collapsing Transition. *Phys. Rev. Lett.*, **72**:041803, 2005.
- [12] I. Kulic and H. Schiessel. DNA Spools under Tension. *Phys. Rev. Lett.*, **92**:228101, 2004.
- [13] F. Solis and M. Olvera de la Cruz. Collapse of Flexible Polyelectrolytes in Multivalent Salt Solutions. *J. Chem. Phys.*, **112**:2030, 2000.
- [14] T. Nguyen, I. Rouzina, and B. Shklovskii. Reentrant condensation of DNA induced by multivalent cations. *J. Chem. Phys.*, **112**:2562, 2000.
- [15] F. Solis and M. Olvera de la Cruz. Flexible Linear Polyelectrolytes in Multivalent Salt Solutions: Solubility Conditions. *European Physics J. E*, **4**:143, 2001.
- [16] V. Bloomfield. DNA condensation by multivalent cations. *Biopolymers*, **354**:269, 1997.

- [17] V. Bloomfield. DNA condensation. *Curr. Opinion Struct. Biol.*, **6**:334, 1996.
- [18] W. Earnshaw, and S. Harrison. DNA arrangement in isometric phage heads. *Nature (London)*, **268**:598, 1977.
- [19] L. Black, W. Newcomb, J. Boring, and J. Brown. Ion Etching of Bacteriophage T4: Support for a Spiral-Fold Model of Packaged DNA. *Proc. Natl. Acad. Sci USA*, **82**:7960, 1985.
- [20] N Hud. Double-stranded DNA organization in bacteriophage heads: an alternative toroid-based model. *Biophys. J.*, **69**:1355, 1995.
- [21] I. Kulic, D. Andrienko, and M. Deserno. Twist-bend instability for toroidal DNA condensates. *Europhys. Lett.*, **67**:418, 2004.
- [22] J. Widom, and RL Baldwin. Cation-induced toroidal condensation of DNA studies with $Co^{3+}(NH_3)_6$. *J Mol Biol.*, **144**:431, 1980.
- [23] AZ. Li, TY. Fan, and M. Ding. Formation study of toroidal condensation of DNA. *Sci China B.*, **35**:169, 1992.
- [24] V. Bloomfield. Condensation of DNA by multivalent cations: Considerations on mechanism. *Biopolymers*, **31**:1471, 1991.
- [25] V. Vijayanathan, T. Thomas, A. Shirahata, and T. J. Thomas. DNA Condensation by Polyamines: A Laser Light Scattering Study of Structural Effects. *Biochemistry*, **40**:13644, 2001.
- [26] T. Kral, M. Hof, and M. Langner. The Effect of Spermine on Plasmid Condensation and Dye Release Observed by Fluorescence Correlation Spectroscopy. *Biol. Chem.*, **40**:331, 2002.
- [27] D. Porschke. Dynamics of DNA Condensation. *Biochemistry*, **23**:4821, 1984.

- [28] D. Chatteraj , L. Gosule, and J. Schellman. DNA condensation with polyamines. 2. Electron microscopic studies. *J. Mol. Biol.*, **121**:327, 1978.
- [29] S. Hamilton and D. Pettijohn. Properties of condensed bacteriophage T4 DNA isolated from Escherichia coli infected with bacteriophage T4. *J Virol.*, **19**:1012, 1976.
- [30] L. Gosule and J. Schellman. Compact form of DNA induced by spermidine. *Nature.*, **29**:259, 1976.
- [31] Z. Lin, C. Wang, X. Feng, M. Liu, J. Li, and C. Bai. The observation of the local ordering characteristics of spermidine-condensed DNA: atomic force microscopy and polarizing microscopy studies. *Nucleic Acids Res.*, **26**:3228, 1998.
- [32] P. Arscott , A. Li, and V. Bloomfield. Condensation of DNA by trivalent cations. 1. Effects of DNA length and topology on the size and shape of condensed particles. *Biopolymers*, **30**:619, 1990.
- [33] M. Haynes, R. Garrett, and W. Gratzer. Structure of nucleic acid-poly base complexes. *Biochemistry*, **9**:4410, 1970.
- [34] M. Hsiang, and R. Cole. Structure of histone H1-DNA complex: effect of histone H1 on DNA condensation. *Proc. Natl. Acad. Sci. USA*, **74**:4852, 1977.
- [35] N. Hud, M. Allen, K. Downing, J. Lee, and R. Balhorn. Identification of the elemental packing unit of DNA in mammalian sperm cells by atomic-force microscopy. *Biochem. Biophys. Res. Commun.*, **193**:1347, 1993.
- [36] U. Laemmli. Characterization of DNA condensates induced by poly(ethylene oxide) and polylysine. *Proc. Natl. Acad. Sci. USA*, **72**:4288, 1975.

- [37] M. Cerritelli, N. Cheng, A. Rosenberg, C. McPherson, F. Booy, and A. Steven. Encapsidated conformation of bacteriophage T7 DNA. *Cell. Proc. Natl. Acad. Sci. USA*, **91**:271, 1997.
- [38] <http://www.fda.gov/cber/gene.htm>
- [39] Y. Yoshikawa, K. Yoshikawa, and T. Kanbe. Formation of a Giant Toroid from Long Duplex DNA. *Langmuir.*, **15**:4085, 1999.
- [40] M. Frank-Kamenetskii, V. Anshelevich, and A. Lukashin. Polyelectrolyte Model of DNA. *Sov. Phys. Uspekhi*, **30**:317, 1987.
- [41] E. Rajasekaran and B. Jayaram. Counterion condensation in DNA systems: The cylindrical Poisson-Boltzmann model revisited. *Biopolymers*, **34**:443, 2004.
- [42] M. Manning. Limiting Laws and Counterion Condensation in Polyelectrolyte Solutions I. Colligative Properties. *J. Chem. Phys.*, **51**:924, 1969. 1969.
- [43] M. Manning. Limiting laws and counterion condensation in polyelectrolyte solutions. IV. The approach to the limit and the extraordinary stability of the charge fraction. *Biophys Chem.*, **7**:95, 1977.
- [44] C. Anderson, M. Record. Polyelectrolyte Theories and their Applications to DNA. *Jr. Annu. Rev. Phys. Chem.*, **33**:191, 1982.
- [45] E. Kramarenko, A. Khokhlov, and K. Yoshikawa. Collapse of Polyelectrolyte Macromolecules Revisited *Macromolecules.*, **30**:3383, 1997.
- [46] R. Winkler, M. Gold, and P. Reineker. Collapse of Polyelectrolyte Macromolecules by Counterion Condensation and Ion Pair Formation: A Molecular Dynamics Simulation Study. *Phys. Rev. Lett.*, **80**:3731, 1998.

- [47] M. Stevens, K. Kremer. The nature of flexible linear polyelectrolytes in salt free solution: A molecular dynamics study. *J. Chem. Phys.*, **103**:1669, 1995.
- [48] R. Dias, A. Pais, B. Lindman, and M. Miguel. Modeling of DNA Compaction by Polycations. *J. Chem. Phys.*, **119**:8150, 2003.
- [49] P. Crozier and M. Stevens. Simulations of single grafted polyelectrolyte chains: ssDNA and dsDNA. *J. Chem. Phys.*, **118**:3855, 2003.
- [50] M. Stevens, K. Kremer. Structure of salt-free linear polyelectrolytes. *Phys. Rev. Lett.*, **71**:2228, 1993.
- [51] M. Stevens, K. Kremer. Structure of salt-free linear polyelectrolytes. *J. Chem. Phys.*, **103**:1669, 1995.
- [52] M. Jonsson, and P. Linse. Polyelectrolyte-macroion complexation. II. Effect of chain flexibility. *J. Chem. Phys.*, **115**:10975, 2001.
- [53] A. Pais, M. Miguel, P. Linse, and B. Lindman. Polyelectrolytes confined to spherical cavities. *J. Chem. Phys.*, **117**:1385, 2002.
- [54] PY. Hsiao. Linear polyelectrolytes in tetravalent salt solutions. *J. Chem. Phys.*, **124**:044904, 2006.
- [55] PY. Hsiao. Chain morphology, swelling exponent, persistence length, like-charge attraction, and charge distribution around a chain in polyelectrolyte solutions: effects of salt concentration and ion size studied by molecular dynamics simulations. *Macromolecules.*, **39**:7125, 2006.
- [56] Stevens M. Simple simulation of DNA condensation. *Biophys J.*, **80**:130, 2001.

- [57] Ou Zhaoyang and M. Muthukumar. Langevin dynamics of semiflexible polyelectrolytes: Rod-toroid-globule-coil structures and counterion distribution. *J. Chem. Phys.*, **123**:074905, 2005.
- [58] I. Miller, M. Keentok, G. Pereira, D. Williams. Semiflexible polymer condensates in poor solvents: Toroid versus spherical geometries. *Phys. Rev. E*, **71**:031802, 2005.
- [59] Y. Takenaka, K. Yoshikawa, Y. Yoshikawa, Y. Koyama, T. Kanbe. Morphological variation in a toroid generated from a single polymer chain. *J. Chem. Phys.*, **123**:014902, 2005.
- [60] SB. Smith , L Finzi , C. Bustamante. Direct mechanical measurement of the elasticity of single DNA molecules by using magnetic beads. *Science*, **258**:1122, 1992.
- [61] SB. Smith , Y. Cui , C. Bustamante. Overstretching B-DNA: the elastic response of individual double-stranded and single-stranded DNA molecules. *Science*, **271**:795, 1996.
- [62] HG. Hansma. Properties of biomolecules measured from atomic-force microscope images: a review. *J. Struct. Biol.*, **119**:99, 1997.
- [63] C. Bustamante, J. F. Marko, E. D. Siggia, and S. Smith. Entropic elasticity of λ -phage DNA. *Science.*, **265**:1599, 1994.
- [64] M D Wang, H Yin, R Landick, J Gelles, and S M Block. Stretching DNA with optical tweezers. *Biophys J.*, **72**:1335, 1997.
- [65] Q. Liao, A. Dobrynin, and M. Rubinstein. Molecular Dynamics Simulations of Polyelectrolyte Solutions: Nonuniform Stretching of Chains and Scaling Behavior. *Macromolecules.*, **36**:3386, 2003.

- [66] R. Zhang and B. Shklovskii. The pulling force of a single DNA molecule condensed by spermidine. *Physica A*, **349**:563, 2005.
- [67] F. Ritort, S. Mihardja, S. B. Smith, and C. Bustamante. Condensation transition in DNA-Polyaminoamide dendrimer fibers studied using optical tweezers. *Phys. Rev. Lett.*, **96**:118301, 2006.
- [68] R. Franklin and R. Gosling. Molecular Configuration in Sodium Thymonucleate. *Nature*, **171**:740, 1953.
- [69] D. Elson and E. Chargaff. On the desoxyribonucleic acid content of sea urchin gametes. *Experientia*, **8**:143, 1952.
- [70] E. Chargaff, R. Lipshitz, and C. Green. Composition of the desoxypentose nucleic acids of four genera of sea-urchin. *J Biol Chem.*, **195**:155, 1952.
- [71] E. Chargaff, R. Lipshitz, C. Green, and M. Hodes. The composition of the deoxyribonucleic acid of salmon sperm. *J Biol Chem.*, **192**:223, 1951.
- [72] E. Chargaff, R. Lipshitz, C. Green, and M. Hodes. Some recent studies on the composition and structure of nucleic acids. *J Cell Physiol Suppl.*, **38**:41, 1951.
- [73] B. Magasanik, E. Vischer, R. Doniger, D. Elson, and E. Chargaff. The separation and estimation of ribonucleotides in minute quantities. *J Biol Chem.*, **186**:37, 1950.
- [74] E. Chargaff. Chemical specificity of nucleic acids and mechanism of their enzymatic degradation. *Experientia*, **6**:201, 1950.
- [75] R. Hockney, and J. Eastwood. Computer simulation using particles. McGraw-Hill, New York, 1981.

- [76] Oppenheim, A. V. and R.W. Schaffer. Discrete-Time Signal Processing. Englewood Cliffs, NJ: Prentice-Hall, 1989.
- [77] Kenneth Barbalace <http://klbprouctions.com/> Periodic Table of Elements, Sorted by Ionic Radius. EnvironmentalChemistry.com. 1995 - 2007. Accessed on-line: <http://EnvironmentalChemistry.com/yogi/periodic/ionicradius.html>
- [78] E. Clementi and D. L. Raimondi. Atomic Screening Constants from SCF Functions. *J. Chem. Phys.*, **39**:2686, 1963.
- [79] J. Slater. Atomic Radii in Crystals. *J. Chem. Phys.*, **41**:3199, 1964.
- [80] J. Widom and R. L. Baldwin. Cation-induced toroidal condensation of DNA: Studies with $Co^{3+}(NH_3)_6$ *J. Mol. Biol.*, **144**:431, 1980.
- [81] Y. Murayama, H. Wada, and M. Sano. Internal Friction of a Single Condensed DNA: Dynamic Force Measurements Using Optical Tweezers. Unpublished paper.
- [82] N. K. Lee and D. Thirumalai. Pulling-Speed-Dependent Force-Extension Profiles for Semiflexible chains *Biophys J.*, **86**:2641, 2004.
- [83] M. Saminathan, T. Antony, A. Shirahata, L. H. Sigal, T. Thomas, and T. J. Thomas. Ionic and Structural Specificity Effects of Natural and Synthetic Polyamines on the Aggregation and Resolubilization of Single-, Double-, and Triple-Stranded DNA. *Macromolecules.*, **28**:8759, 1995.
- [84] O. Kratky, and G. Porod. Röntgenuntersuchung gelöster Fadenmoleküle *Rec. Trav. Chim. Pays-Bas.*, **68**:1106, 1949.
- [85] J. Marko and E. Siggia. Stretching DNA. *Macromolecules.*, **28**:8759, 1995.

- [86] T. Odijk. Stiff chains and filaments under tension. *Macromolecules.*, **28**:7016, 1995.
- [87] C. Bouchiat, M. Wang, J. Allemand, T. Strick, S. Block, and V. Croquette. Estimating the persistence length of a worm-like chain molecule from force-extension measurements. *Biophys J.*, **76**:409, 1999.

